Trajectory Specification to Support High-Throughput Continuous Descent Approaches

by

Titilayo Fasoro

Submitted to the Department of Aeronautics and Astronautics
in partial fulfillment of the requirements for the degree of

Master of Science in Aeronautics and Astronautics

at the

MASSACHUSETTS INSTITUTE OF TECHNOLOGY

May 2022

Author .....
Department of Aeronautics and Astronautics
May 17, 2022

Certified by .....
Hamsa Balakrishnan
Professor of Aeronautics and Astronautics
Thesis Supervisor

Accepted by .....
Jonathan P. How
R. C. Maclaurin Professor of Aeronautics and Astronautics Chair,
Graduate Program Committee

Trajectory Specification to Support High-Throughput Continuous Descent Approaches

by

Titilayo Fasoro

Submitted to the Department of Aeronautics and Astronautics
on May 17, 2022, in partial fulfillment of the
requirements for the degree of
Master of Science in Aeronautics and Astronautics

Abstract

Continuous descent approaches (CDAs) have demonstrated the ability to reduce aircraft fuel burn and noise, while trajectory-based operations (TBO) have been shown to improve the predictability and throughput of aircraft flows. Prior work has recognized the difficulty of implementing CDAs in high-density terminal areas due to an increase in uncertainty, which can result in a decrease in throughput. This thesis investigates whether increased throughput afforded by trajectory-based operations can be combined with continuous descent approach profiles to achieve high-throughput CDA operations. The proposed method in this thesis first determines a CDA profile via trajectory optimization, and then locates waypoints with required time of arrival (RTA) constraints along this profile, to optimize a combination of throughput and fuel burn. For representative terminal-area descent profiles at Hartsfield-Jackson Atlanta International Airport (ATL), we find that by specifying intermediate waypoints with RTAs, it is possible to use intermediate waypoints with RTAs to increase the throughput by as much as 70%, while incurring an additional fuel burn penalty of 2% per flight.

Thesis Supervisor: Hamsa Balakrishnan
Title: Professor of Aeronautics and Astronautics

Acknowledgments

First and foremost, I am grateful to God for bringing me this far, from the start of my Masters degree to the writing of this thesis.

Next, I would like to thank my amazing advisor Prof. Hamsa Balakrishnan for her endless support and guidance through every step of this project. In addition to the multiple feedback and encouragement I received, her invaluable insights in research directions and study materials helped shaped the development of this work. Without her this thesis will not have come to fruition. I am extremely grateful for all the ideas and research meetings, being always ready to answer my questions and give relevant feedback. I am also indebted to Sandeep and Dun Yan for their previous research that provided inspiration for my project.

I also want to extend my gratitude towards the MathWorks founder Jack Little for the fellowship assistance during the second year of my degree. I am extremely grateful for not having to worry about funding during that period, it was because of this that I was able to fully dedicate my time to this research.

I am also grateful for the support resources at the AeroAstro department for helping me through the times I faced health problems and had deadlines to complete.

I want to also take this opportunity to thank my friends for their emotional support during stressful times, all the lunch breaks and eating out were stress-relieving.

Last but certainly not the least, I would love to thank my family for their prayers, support and encouragement throughout the stressful and challenging times in completing my degree and taking classes. I am thankful for my parents for calling frequently to ask about my well-being as well as my siblings being ready to lend an ear and provide me with whatever I needed.

Contents

List of Figures

List of Tables

Chapter 1

Introduction

1.1 Motivation

Excluding the pandemic period, the International Civil Aviation Organization (ICAO) reports that the air transport industry doubled every 15 years, and is expected to double over the next two decades with a yearly growth rate of about 4 percent [1, 2]. In the United States alone, the Bureau of Transportation Statistics (BTS) estimated an increase of 140 million enplanements in 2017 compared to the previous five years [3]. Similarly, Europe has experienced a record high of 11 million flights in 2018 with expected 15 million per year by 2035 [4–6], while the Asian and Pacific regions are expected to experience the highest passenger traffic growth rates in the world. This growth in traffic, along with the increase in other forms of flight caused by the booming drone industry, will bring about challenges such as increased delays, and more air and noise pollution. If measures are not put in place, current aviation technology may not be able to accommodate such changes even in the absence of environmental constraints. Moreover, given that airplane fuel alone makes up about 20% of airline operating costs and expected to increase yearly [7, 8], there is much inclination for airlines to study ways of increasing fuel efficiency and reducing fuel consumption. Apart from economical incentives, global warming concerns outlined by the ICAO's future emission goals has prompted the aviation industry to realize solutions to eliminate environmental impact [9]. Such concerns arise from the fact

that the aviation industry currently accounts for approximately 2% of man-made global CO2 emissions [10, 11], in addition to effects from contrail formation and other gases like NOx and CO black carbon [12, 13].

The need for increasing airspace capacity while reducing environmental impact has been the driving force of air transportation system modernization efforts. Current research methods focus on generating efficient aircraft operations that reduce environmental impacts and costs without compromising on capacity and safety. These issues have been identified by the ICAO's Global Air Navigation Plan (GANP) whose member states include the Single European Sky ATM Research (SESAR) in Europe [4], Next Generation Air Transport System (NextGen) in the United States [14], Australian ATM Strategic Plan (AATMSP) in Australia [15], and Collaborative Actions for Renovation of Air Traffic Systems (CARATS) in Japan [16]. A common aspect of these programs is the paradigm shift from open-loop vectoring to trajectory-based control by implementing 4D trajectories in all phases of the flight; commonly known as 4D Trajectory Based Operations (TBO). In the same field of vision, Continuous Descent Approaches (CDAs) have been proposed to provide efficient trajectories at Terminal Maneuvering Areas (TMAs) [17]. Much attention has been drawn to making the arrival management process more efficient, but it remains challenging due to difficulty in merging flows and meeting capacity constraints without sacrificing fuel costs. CDA enabled by time-managed 4D generated trajectories has been considered as a promising solution. CDA will allow for less environmental impact and fuel costs, while time-based management near the terminal airspace will increase predictability.

1.2 Continuous Descent Approaches

Conventional aircraft descent methods are designed with multiple level-offs to meet path constraints and ensure proper spacing between aircraft while resolving conflicts and managing traffic flow. These profiles are usually achieved by the Air Traffic Controller (ATC) assigning multiple altitude clearances and/or speed adjustments that often achieve maximum runway capacity but tend to worsen performance. Further-

more, in high demand scenarios, arriving aircraft may spend long periods in holding patterns at low altitudes, incurring even more fuel costs. Continuous Descent Arrival (CDA) also known as Continuous Descent Operation (CDO) or Optimized Profile Descent (OPD) is one of the concepts proposed to provide efficient descent trajectories by the ICAO's Global Air Navigation Plan (GANP) program [18]. In contrast to conventional approach procedures, CDA maintains idle/near-idle thrust while descending from the cruise altitude until the final glide slope, reducing the amount of level-offs and allowing the aircraft to fly at optimal speeds. In addition to fuel cost reduction, flying closer to the ground for less time periods lowers the amount of noise generation at locations around airports. An Optimized Profile Descent (OPD) is a type of CDA where the descent profile is accompanied by a STAR profile. The rest of this thesis will use the terms CDA and OPD interchangeably.

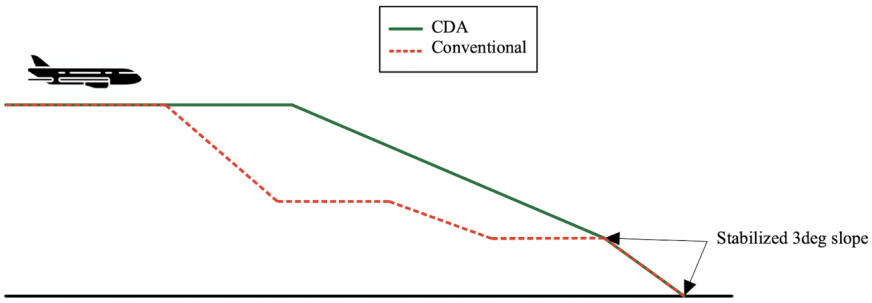

Figure 1-1: CDA concept Illustration

Nowadays CDAs have been introduced at a number of airports, being performed most of the time at airports with little to no traffic and only during off-peak times at specific busy airports [19]. Even though a perfect CDA happens from the top of descent to runway, airspace limitations may prevent that in actual operations. In such cases, it is possible to complete a CDA up to the limitation segment and continue afterwards till touchdown [20]. Various studies and flight trials have demonstrated CDA benefits as a fuel-saving procedure capable of reducing emissions and noise pollution [21–29]. In 2007, flight tests at Los Angeles International Airport revealed an average saving of 25 gal of jet fuel per flight or "annual reduction of 2,000,000 gal

of jet fuel and 41,000,000 lb of carbon dioxide emissions" [21]. Similar flight trials showed a 25-40% reduction in fuel consumption in the last 45 kilometers at Schiphol Airport [22], and 56kg fuel savings for every flight compared with conventional at Stockholm Arlanda Airport [24]. As investigated in [30], the theoretical justification for why CDA saves fuel is mainly due to its elevated altitude idle thrust setting. In short, fuel burned over a time period increases with altitude for low speeds but decreases with altitude for high speeds . By allowing the aircraft to fly higher speeds at higher altitudes, the speed profile is closer to its fuel-optimal form.

Implementing CDA remains challenging as requiring each aircraft to continuously descent for the sake of saving fuel will induce a large amount of trajectory uncertainty. This predictability is caused by the variability in CDA profiles due to a wide range of factors like flight path angle [31], weather and structure of the aircraft [32–34]. Airports with less traffic may allow CDAs to be performed, but in high-density operations where potential benefits of CDA are maximized, additional space will have to be sectioned during descent to ensure safe separation while maintaining an uninterrupted descent, thus leading to lower airport throughput. Therefore, understanding uncertainty during CDA operations will be beneficial in improving aircraft safety, capacity, and efficiency. The research on enabling CDA implementation has been inspired a few methods to reduce uncertainty and handle aircraft spacing/merging including altitude windows [35], Tool for Analysis of Separation and Throughput (TASAT) [36], the Time Space Diagram (TSD) [37], fixed path angle [38], arrival time controllability [39–43] and other analytical methods [44]. For the purposes of this research, to handle the difficulty of CDA in control operations, arrival time controllability in form of time constraints will be explored.

1.3 Trajectory-Based Operations

Inefficiencies in the current air traffic architecture arise due to limited shared information between Air Traffic Controllers (ATCs), as well as downstream flows caused by delays and re-routing. These factors motivate development of techniques that

delegate more controller workload to automation, enabling ATCs to control aircraft streams instead of individual crafts. One of the main solutions to increase capacity and safety while reducing environmental impact is moving from clearance-based ATC to trajectory-based ATC operations. Trajectory Based Operations (TBO) is a key element of this change which according to NextGen Implementation involves "strategically planning, managing, and optimizing flights throughout the operation using time-based management, information exchange between air and ground systems, and an aircraft's ability to fly precise paths in space and time" [14]. Moving from the traditional clearance-based control to trajectory-based control will enable user-preferred optimal 4D trajectories to be flown from gate to gate. Such trajectories are negotiated between airlines and the ATM system in order to satisfy operational requirements such as reduced fuel consumption. A crucial component to achieve this is not only the aircraft's ability to construct a 4-D trajectory, but also precisely follow the planned path. The main method of constructing planned 4D trajectories and closed loop control to track them is the Flight Management System (FMS) of the aircraft.

Implementing TBO may constitute time based metering to monitor 4D trajectories (4DT) defined in space. Defining a 4DT with time metering involves specifying a sequence of 3D spatial aircraft waypoints each associated with a Required Time of Arrival (RTA). This RTA requirement is met by an advanced FMS time-control functionality which adjusts the aircraft's speed control to eliminate the difference between its estimated time of arrival (ETA) and RTA. Incorporating such a concept into current Air Traffic Control (ATC) procedures will require advanced FMS capabilities, improved Data communication and ADS-B services on aircraft [45]. According to SESAR, performing TBO will require exchange of updated 4D flight information between all authorized stakeholders via a System Wide Information Management (SWIM) [4, 45]. Additionally, concepts like Aircraft Intent Description Language (AIDL) to describe and exchange aircraft predicted aircraft trajectories in an interoperable manner [46] and ground-based automation to assist with separation and flow will be key enablers for this operation [47].

Although the concept of 4DT has been around for a long time, there is room for research on its architecture and applications such as aircraft merging, sequencing, deconflicting, spacing requirements, and so on. Many of the design aspects of 4DT being investigated by researchers often involve queuing techniques [48, 49], sequencing/scheduling methods [50, 51], conflict resolution [52, 53], optimizing merging techniques [54–56], calculating metering accuracy, estimating feasible RTA time window for metering operation [57], optimizing speed profiles affected by meteorological factors [58–60], and computing uncertainties in the design that arise from external factors [61]. Time-managed 4DT flight trials have also taken place to examine the factors that affect RTA functionality. A number of them have identified wind forecast error [62–64], navigation, flight technical and modeling errors [58, 64], location of initial flap deployment [63], difference in the time constraint from the optimal time-of-arrival [63], as well as delayed level clearances to have significant influence on RTA uncertainties. Efforts to quantify such uncertainties, as well as control policies to correct them are topics of interest to many [57, 63, 65–71].

Assigning a time constraint of a 4DT arrival is one of the proposed solutions to improve the lack of predictability experienced in CDA operations. However, unlike the cruise phase of the flight, time control is more limiting during descent since the available speed windows are smaller at lower altitudes [32]. This calls for informed decisions on the choice of RTA values to prevent spacing infringement and properly scheduling their arrivals. For aircraft with RTA functionality, an ATC implementation would resemble controlling traffic flow by assigning RTAs at/near the runway to each incoming aircraft in advance.

1.4 Related Work

1.4.1 CDA Profile Design

Designing an optimized descent profile is one of the cornerstones of facilitating CDA in the terminal space area. Numerous studies have investigated the use optimization

techniques to design CDAs in form of an aircraft flight planning problem [26,39,41,54, 72–82]. Elements of the flight planning problem generally include an aircraft performance model (APM), wind model if wind is present, a cost function that defines the parameters to be minimized, and path/performance constraints. The APM describes the aircraft's dynamics and kinematics with three or six degrees of freedom [75,82] depending on what displacement directions and means of control are of interest. A few optimization problems optimize the entire 4 dimensional trajectory, but most APM models only focus on longitudinal and altitude directions, and in come cases time. In addition to this, a few papers extend the APM model by applying stochastic aircraft dynamics [83] for applications like probabilistic conflict detection and resolution.

The wind model on the other hand may have a uniform value for the entire trajectory, consist of historical realistic data [84], or based on a probabilistic model such as [81,82] which uses a Global Ensemble Forecast System (GEFS). Constraints on the flight trajectory range from very flexible but reasonable flight limitations [81] to adhering to actual STAR waypoints at an airport [82]. [80] for example consists of only two phases with very generous constraints while [75] uses STAR waypoint limitations to design all 3 dimensions of an 8-phase flight. A few others also take this further by designing the entire flight trajectory from take-off to landing [79] or re-optimizing the trajectory after aircraft deviates from its planned [59, 85, 86], but these topics are outside the scope of this thesis. Lastly, cost parameters include time, fuel, noise, and path uncertainty.

Typical analytical methods formulate trajectory optimization as a Non-Linear Programming (NLP) problem. Numerical methods of solving optimal control problems include direct, indirect and dynamic programming. Direct collocation methods are the most popular choice of solution approach, and are adopted in this thesis. In addition to solving the trajectory optimization problem much work has been done to examine the effects of wind variation, flight path angle and location of top of descent on CDA profile to design robust trajectories [77, 80–82] .

1.4.2 Arrival Time Controllability

As previously mentioned, having time controllability while performing a CDA profile may not only improve trajectory predictability, but also ensure proper aircraft separation, manage conflicts, and better runway throughput. Numerous field trials and simulation results have demonstrated use of RTA functionality to assist aircraft performing CDA [16, 19, 32, 39, 41–43, 51, 87–96]. A few accomplish this by adding a time-based parameter in the cost function of CDA trajectory optimization problem while a few others set a fixed RTA constraint at the end of the trajectory planning problem. An example is the time and energy managed operations (TEMO) concept which uses an energy modulation algorithm to efficiently meet an assigned RTA with idle thrust by exchanging potential and kinetic energy of the aircraft [92, 97, 98]. Another method is presented in [19, 90, 91] as a control design named "Optimal E*" that constructs fuel-efficient RTA-complaint 4-dimensional trajectories accounting for wind errors. Optimizing using a time constraint has been extensively researched to the extent that planning robust trajectories in all 4 dimensions of the flight being applied to airport procedures is possible [75, 82].

Further evaluations of arrival-time controllability experiments reveal limitations in this method and operational issues to be solved. Many of these investigations identified wind error being the main contribution to deviation from assigned time in addition to speed/altitude constraints and flap schedules/landing configuration extension [66]. The wind error significance was further explained in the flight trials [32] which discovered that wind uncertainties accumulate more later in the descent owing to speed windows being less constrained at higher altitudes, thus attaining more flexible control at a higher elevation.

Not only operational issues are being identified, but comparisons and trade-off analysis to propose solution methods for improving accuracy. [72] observed the trade-off between fuel savings and trajectory predictability (in form of feasible RTA window) by examining latest and earliest trajectories. Likewise, [99] conducted a sensitivity study to realize the impact of issuing sub-optimal RTAs, different cost indexes, and

distances to the RTA fix. RTA was found to incur more costs as opposed to unrestricted operations and less compared to level-offs. Given that an aircraft can fly powered descents or add path stretches to meet a RTA, [96] compared the costs between both methods and recognized that although path stretches initially burns more fuel, it consumes less in the longer run. In addition to these revelations, time-control use has been applied to airplane scheduling, conflict detection and spacing. Examples include using mixed integer programming methods to schedule simulated time-constrained CDA profiles [51,100], solve an aircraft landing problem [95], manage separation [101], or dynamic programming to monitor spacing between aircraft [102,103].

1.5 Thesis Contributions

Although there has been much discussion about time-compliant CDA profiles, most of the work done in the past focuses on implementing only one RTA constraint along the trajectory. [15] used multiple waypoints, but only for a fixed small number and did not give the implications from applying multiple versus only one. [102, 103] designed multiple metering points, but it was to ensure enough spacing and not to meet time constraints. This research assesses the implications of executing multiple RTAs on a CDA trajectory in addition to what trade-offs need to be made. Instead of using level-offs to merge aircraft, solve conflicts and manage uncertainty, RTAs placed at intermediate points along the trajectory will accomplish that. Although RTAs are most effective for longer time horizons, using shorter time horizons may be needed in high-demand situations when there is less concern on fuel savings. The paper will begin by describing the CDA profile to be used, followed by the method of measuring uncertainty in the given trajectories. Then a framework on optimal placement of RTA metering fixes will be described. Finally, a trade-off study will be between predictability, throughput and potential fuel savings from CDAs will be performed.

Chapter 2

Vertical Trajectory Optimization

In this chapter, the methodology of designing a CDA trajectory that minimizes fuel consumption and total time elapsed is introduced. In practice, the optimized profile represents the aircraft's route in the flight planning phase agreed between the airline and aviation stakeholders. As detailed in the relative work section, approaches have been explored to solve this problem using various control and operational parameters. Most methods minimize parameters like fuel burn, time, noise and emission costs using control options such as throttle setting, flight path angle, speed brakes deflection and load factor [41, 77, 95–97]. The optimization problem presented in this research uses elevator-controlled flight path angle (to modulate energy) and engine thrust (to add or subtract energy) as the control options to minimize fuel burn and time. Designing a flight plan assumes a scenario where the pilots have almost completed the cruise portion of the flight and are about to execute the descent portion. The cruise portion is included in the optimization problem to determine the top of descent (TOD) and to give enough control authority for the aircraft to meet an assigned time constraint. Based on current piloting procedures, the profile constraints are selected with respect to constant Calibrated Air Speed (VCAS) and Mach number M. Moreover, the fixed lateral portion of the flight is assumed to be known as determined by Standard Terminal Approach Route (STAR) procedures, while the final time is located at the Initial Approach Fix or Final Approach Fix (IAF/FAF). The path constraints turn the design problem into a trajectory optimization with multiple phases which can be

solved with a nonlinear programming tool.

2.1 Aircraft Dynamic Model

The Flight Management System (FMS) of an aircraft may use a trajectory predictor to determine the vertical profile to fly by numerical integration of aircraft model equations. To find a balance between accuracy and computational efforts, the selected equations of motion are modelled as a simplified 3-DOF point-mass aircraft model controlled by control inputs represented by the following ordinary differential equations [104]:

$$\dot{V} = \frac{T - D}{m} - g \sin \gamma \tag{2.1}$$

$$\dot{d} = V \cos \gamma + U_w \tag{2.2}$$

$$\dot{h} = V \sin \gamma \tag{2.3}$$

$$\dot{m} = -\dot{F}_{fuel}(T, h) \tag{2.4}$$

where the states V, d, h and m represent true air speed (TAS), along track position, altitude, and aircraft mass respectively. The flight path angle γ and thrust T are selected as the control inputs to the problem. The following assumptions are made in the equations [135]:

1. Thrust vector is parallel to the aerodynamic velocity of the aircraft [34]
2. Symmetric flight
3. Flight path angle consists of very small values, therefore its change is assumed to be minimal ($\dot{\gamma} \approx 0$)
4. Vertical wind component neglected due to its low influence on geodetic altitudes below 35000ft [105]
5. Steady wind conditions ($\dot{U_w} \approx 0$)

6. Continuous vertical equilibrium is assumed, making the lift force equal (expressed in Equation 2.5) to the gravity force.

$$L = mg\cos(\gamma) \tag{2.5}$$

A North-east down frame is used to describe the coordinate system, and the International Standard Atmosphere (ISA) model is applied in determining altitude-varying parameters such as temperature, density, and pressure.

For Equation 2.1, the drag force can be written in terms of dynamic pressure and drag coefficient which can be further expressed in terms of lift coefficient and drag polar.

$$D = C_D \frac{1}{2} \rho V^2 S \tag{2.6}$$

$$C_D = C_{D0} + kC_L^2; \tag{2.7}$$

$$C_L = \frac{L}{\frac{1}{2}\rho V^2 S} = \frac{mg\cos\gamma}{\frac{1}{2}\rho V^2 S} \tag{2.8}$$

The required parameters wing area S, drag coefficients zero-lift (C_{D0}) and lift-induced (k) are provided by an open-source aircraft performance model OpenAP [106] for a variety of aircraft types and based on their configuration. Furthermore, the nominal fuel flow rate $\dot{F}_{fuel}$, can be written in terms of thrust T and altitude h according to the OpenAP model:

$$T_{avg} = \frac{T}{\text{number of engines}} \tag{2.9}$$

$$\dot{F}_{fuel}(T,h) = C_{ff,3}\left(\frac{T_{avg}}{T_0}\right)^3 + C_{ff,2}\left(\frac{T_{avg}}{T_0}\right)^2 + C_{ff,1}\left(\frac{T_{avg}}{T_0}\right) + C_{ff,ch}\cdot T_{avg}\cdot h$$

where T_0 is the maximum static thrust for at sea-level and, C_{ff1}, C_{ff2}, C_{ff3}, and $C_{ff,ch}$ are constant coefficients obtained from OpenAP. This section focuses on the Airbus A320 equipped with a CFM56-5B engine whose coefficient values are summarized in Table 2.1

Parameter	Value	Units
C_{D0}	0.018	-
K	0.039	-
S	124	m^2
T_0	117900.0	N
$C_{\text{ff},3}$	0.410732	-
$C_{\text{ff},2}$	-0.46575	-
$C_{\text{ff},1}$	1.22383	-
$C_{\text{ff},ch}$	5.1e-07	-
# of engines	2	-

Table 2.1: A320 Aerodynamic and Propulsion Parameters

2.2 Trajectory Optimization Formulation

Finding CDA profiles is formulated as an multi-phase constrained optimal control problem with dynamic and terminal constraints. In general, a single phase optimal control problem is expressed as [107]:

$$\begin{aligned}
\min_{\boldsymbol{u}(t)} \quad & J(t, \boldsymbol{x}(t), \boldsymbol{u}(t), p) := l_f(t_f, \boldsymbol{x}(t_f), t_f, p) + \int_{t_0}^{t_f} l(t, \boldsymbol{x}(t), \boldsymbol{u}(t), t, p)\mathrm{d}t \\
\text{subject to} \quad & \dot{\boldsymbol{x}} = \boldsymbol{f}(\boldsymbol{x}(t), \boldsymbol{u}(t), t, p) \\
& \boldsymbol{g}(\boldsymbol{x}(t), \boldsymbol{u}(t), t, p) = 0 \\
& \boldsymbol{\phi}(\boldsymbol{x}(t), \boldsymbol{u}(t), t) \leq 0 \\
& \boldsymbol{e}(t_0, \boldsymbol{x}(t_0), t_f, \boldsymbol{x}(t_f), p) \leq 0 \\
& \boldsymbol{h}(t_0, \boldsymbol{x}(t_0), t_f, \boldsymbol{x}(t_f)) = 0
\end{aligned} \tag{2.10}$$

where $\boldsymbol{x} \in \Re^n$ is the state vector of dimension n, $\boldsymbol{u} \in \Re^m$ is the control vector, $[t_0, t_f]$ is the time horizon between a fixed initial time t_0 and flexible/fixed final time t_f, while p consists of the parameters. The algebraic constraints $\boldsymbol{g}$, path constraints $\boldsymbol{\phi}$, event constraints $\boldsymbol{e}$ and terminal constraints $\boldsymbol{h}$ describe the control problem's boundary conditions. Finding a CDA profile can be formulated as an multi-phase constrained optimal control problem with dynamic and terminal constraints. Given N number of phases, in general, a multi-phase optimal control problem in standard

Bolza form is expressed as [107]:

$$
\begin{aligned}
\min_{\boldsymbol{u}(t)} \quad & J(t, \boldsymbol{x}(t), \boldsymbol{u}(t), p) := \sum_{k=1}^{N} \left[l_f^{(k)}(t_f^k, \boldsymbol{x}^k(t_f^k), t_f^k, p^k) + \int_{t_0^k}^{t_f^k} l^{(k)}(t, \boldsymbol{x}^k(t^k), \boldsymbol{u}^k(t^k), t^k, p^k) dt \right] \\
\text{subject to} \quad & \dot{\boldsymbol{x}^k} = \boldsymbol{f}^{(k)}(\boldsymbol{x}^k(t^k), \boldsymbol{u}^k(t^k), t^k, p^k) \\
& \boldsymbol{g}^{(k)}(\boldsymbol{x}(t^k), \boldsymbol{u}^k(t^k), t^k, p^k) = 0 \\
& \boldsymbol{\phi}^{(k)}(\boldsymbol{x}^k(t^k), \boldsymbol{u}^k(t^k), t^k, p^k) \leq 0 \\
& \boldsymbol{e}^{(k)}(t_0^k, \boldsymbol{x}^k(t_0^k), t_f^k, \boldsymbol{x}^k(t_f^k), p^k) \leq 0 \\
& \boldsymbol{h}^{(k)}(t_0^k, \boldsymbol{x}^k(t_0^k), t_f^k, \boldsymbol{x}^k(t_f^k)) = 0 \\
& \text{for } k = 1, 2, ..., N
\end{aligned}
\tag{2.11}
$$

where $\boldsymbol{x^k} \in \Re^4$ is the vector of the four states in the aircraft dynamic model, $\boldsymbol{u^k} \in \Re^2$ is the control vector of two variables, $[t_0^k, t_f^k]$ is the time horizon in the kth phase, and $\boldsymbol{\phi}$, $\boldsymbol{g}$, $\boldsymbol{\phi}$, $\boldsymbol{e}$ and $\boldsymbol{h}$ consist of all the algebraic, event and terminal constraints. The dynamic constraint $f(x, u, t)$ consists of the aircraft model equations of motion listed in (2.1)-(2.4). Outputs from the optimization include time histories of the state vector $\mathbf{x} = \{V, h, s, m\}$ and control inputs $\mathbf{u} = \{T, \gamma\}$. For this particular problem, the number of phases depends on how many waypoints are in the STAR procedure to be optimized.

2.2.1 Cost Function

The main parameters of interest in this problem are the aircraft's fuel consumption and total time elapsed. Lagrange term in the objective functional and end costs for the optimization problem are formulated as:

$$
J = \sum_{k=1}^{N} \left[\int_{t_0^k}^{t_f^k} \dot{F}_{fuel}^k + C_I^k dt \right], \tag{2.12}
$$

where C_I represents the cost index, and $\dot{F}_{fuel}$ is the nominal fuel flow as described in Equation 2.10. Time-related costs are considered in the cost index C_I term with respect to the fuel consumption costs. The final time at the end of the trajectory

can be either fixed in which case the cost index is zero, or is free to move between two values. One of the additional goals of the optimization problem is to determine where the TOD location, s_{TOD} is. The simplified dynamics in the cruise of the flight restricts the thrust to whatever value the drag is, this allows the top of descent to be determined solely by the horizontal distance covered and cruise velocity.

2.2.2 Constraints

Solving the optimization problem requires satisfying a set of constraints while minimizing the cost functional. These set of constraints are established to resemble current piloting schedules, this will require some knowledge about the limitations of the aircraft and restrictions for waypoints at the terminal manuevering area. These equations can be written as mathematical functions if the control inputs and states.

Control inputs

The boundaries of two control inputs, thrust and flight angle, vary for phases of the flight. Given the type of aircraft and engine, the maximum thrust during cruise and descent can be determined. These values can be obtained from OpenAP's data. Table 2.1 gives the values for a A320 aircraft with a CFM56-5B4 engine. During cruise, a maximum thrust is provided, but since the aircraft is not accelerating during this phase, it is balanced with the amount of drag produed. During descent, the maximum thrust is set to 7% of the maximum thrust setting. However from most of the results, the thrust during descent remains relatively low. Flight angle on the other hand is set to zero in cruise and varies between -6° and 0° while in descent. Flight results mostly indicate that the aircraft flies nearly -3° when descending. This negative values in flight path angle indicates that the thrust produced during descent is less than the total drag, the rest of the drag being compensated by gravity component. This leads to a lower fuel burn and is utlimately one of the reasons why it is desired to elminate level segments during CDA.

Inputs	Min	Max
T (cruise)	0	T_0
T (descent)	0	0.07 T_0
γ (cruise)	0°	0°
γ (descent)	-6°	0°

Table 2.2: Control Input Bounds

Terminal Area Restriction

Most airport terminal areas have Standard Arrival Route (STAR) procedures that describe an airplane's trajectory between its en-route portion and landing approach (E.g. Fig. 4-2). The number of waypoints in such an arrival plan will determine the number of phases and some state constraints in the optimization problem Equation 2.11. Since the states in the problem only focus on the x-z plane, it is also assumed that the aircraft flies latitude and longitude path provided by STAR in the x-y plane. In addition to speed and waypoint positions provided by STAR, flight phases are restricted by constant Calibrated Airspeed (CAS)/Mach number values. For optimized trajectories in this project, speed bounds in first two phases are defined by mach number and the rest by CAS (V_c). For all flights in this study, below FL100 the speed is limited to an indicated air speed of 250 knots (14 CFR § 91.117). Although speed constraints are specified in CAS and Mach number, the equations below can be used to convert them to true airspeed constraints given altitude-dependent parameters:

$$\begin{aligned} q_c &= p_0 \left(\left(\frac{V_c^2}{5a_0^2} + 1 \right)^{\frac{7}{2}} - 1 \right) \\ V(V_c, h) &= 5 \left[\left(\frac{q_c}{p} + 1 \right)^{2/7} - 1 \right] \sqrt{\frac{\rho_0}{\rho}} \\ V(M, h) &= a_0 M \sqrt{\frac{p}{\rho_0}} \cdot \sqrt{\frac{\rho_0}{\rho}} \end{aligned} \tag{2.13}$$

p represents the atmospheric pressure, a the speed of sound, and ρ denotes the air density. $p_0 = 101325$Pa, $a_0 = 343$ m/s, and $\rho_0 = 1.225$kg.m^3 denote the standard values at mean sea level (MSL). Initial conditions for the problem are known since the aircraft makes the CDA optimization after previous flight portions have been

completed. The numerical values used of the velocity constraints are obtained from the OpenAP model [106]. Table 2.3 gives a generalized summary of all the required variable constraints in this problem

Phase	Description	Path Constraints	Final Conditions
c	Cruise	$\mathrm{M}_{\min} \leq M \leq M_{MO}$	
		$\mathrm{h}=\mathrm{h}_0, \gamma = 0^\circ$	
d_1	ToD to ...	$\mathrm{M}_{\min} \leq M \leq M_{MO}$	...
d_2	... to 10000ft	$\mathrm{V}_{\min} \leq V \leq V_{MO}$	...
...	...	...	...
d_N	... to h_{FAF}	...	$\mathrm{h}=\mathrm{h}_{FAF}$

Table 2.3: Constraints Summary

Other Constraints

Not all limitations are specified by the STAR chart. For the safety and comfort of passengers, the maximum acceleration of the aircraft $\dot{V}$ (Equation 2.1) is set to below the BADA manual recommended value of 2.0ft/s [108]. Load factor ($n = \frac{L}{mg}$) is also varied between 0.7 and 1.4 [108].

2.2.3 Computation

The optimization problem, originally written in continuous domain is discretized over finite time at a set of collocation points and solved using nonlinear programming tools. Given different constraints assigned to phases of trajectory, Legendre-Gauss pseudo-spectral methods are used to represent the trajectory solution as a linear combination of polynomial functions and solved using MPOPT, a python module that uses an open-source package called IPOPT for solving multiphase nonlinear optimization problems [107]. The initial guess, number of collocation points and polynomial order are also also chosen. A drawback to this solver was the requirement for the dynamic equations to be written explicitly, potentially posing an issue for altitude-dependent variables such as density and pressure that used python in-built ISA-based functions. This was solved by using polynomial approximations to find relationship between altitude and such dependent variables.

2.3 Factors Affecting CDA Profile

With the trajectory problem clearly defined, parameters can be varied to identify the effects of certain parameters on the CDA profile. This type of analysis can potential be used to perform sensitivity analysis or obtain uncertainty sets when planning a robust CDA trajectory.

2.3.1 Wind Variation

Different wind properties are going to affect the aircraft's trajectory especially the fuel burn. To understand the effect of wind presence, a constant value is assumed for the entire trajectory. Fig. 2-1 shows the effect of winds up to 20kts on speed, altitude and fuel burn. As expected, the top of descent is greatly affected steep the flight path angles, the cruise portion increasing for higher tailwinds and decreasing for stronger headwinds. Fuel burn also increases significantly with stronger tailwind, and the difference in fuel consumption with the baseline scenario much greater with higher tailwind than head wind. This difference is due to the nonlinear relationship between drag and speed.

2.3.2 RTA Variation

When final time is fixed and cost index is set to zero, the time at the end can be set to represent an RTA value. Fig. 2-2 shows the effect of RTA on wind and altitude profile. Larger RTA values have earlier top of descents and lower speed schedules and vice-versa. It is interesting to note that higher RTA speed profiles prefer to initially stay at lower speeds before a surge at the end. The jump at the end also reflects as a level segment in altitude and late surge in fuel consumption, this increase in speed is most likely present to meet the specified RTA on time. It can be inferred that the most optimal choice of RTA for this flight lies somewhere around the first three RTA values, or else the aircraft will have to expend more fuel.

2.3.3 Cost Index

With a flexible final time constraint, the total time is affected by the cost index as shown in Fig. 2-3. This is another method of targeting a selected final time. The speed profile increases for higher CI to make the aircraft reach its destination faster, this in turn moves the ToD earlier and incurs a great amount of fuel cost. Additionally, there a point at which the cruise portion entirely disappears and the aircraft follows the limitations in other phases. This in turn causes a significant amount of fuel burn to happen. Although not displayed, the time at the end for these profiles ranged from 30 minutes (1850s) to 36 mins (2200s). For CI calues less than 1e-2, the RTA values, speed and altitude profiles remained the same.

2.3.4 Distance to Meter Fix

The length of the distance to meter fix had no bearing on the speed profiles (in Fig. 2-4) except increase the fuel burn (as expected). This indicates that any of the distances are sufficient to perform an analysis as long as they remain the same for all the trajectories to be compared.

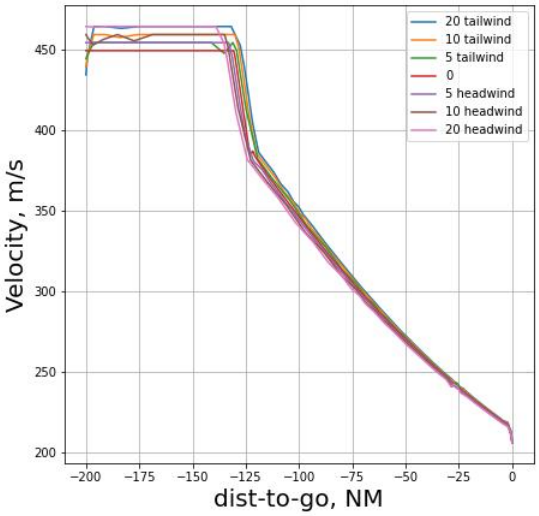

(a) Speed

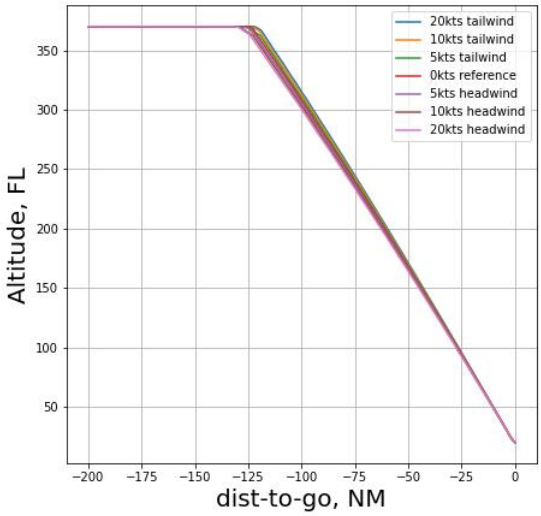

(b) Altitude

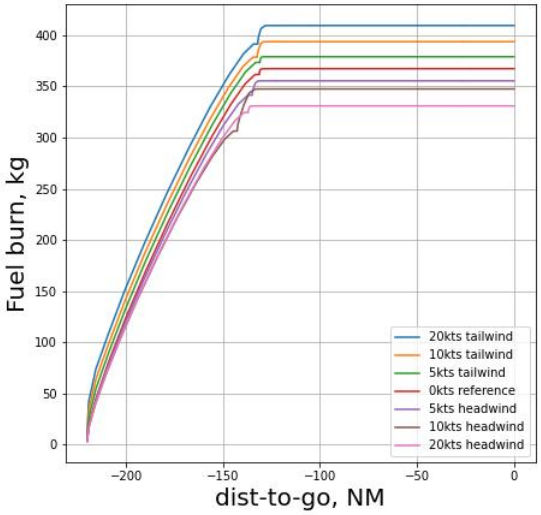

(c) Fuel burn

Figure 2-1: Variation of speed, altitude and fuel burn with distance-to-go, for different values of wind speed.

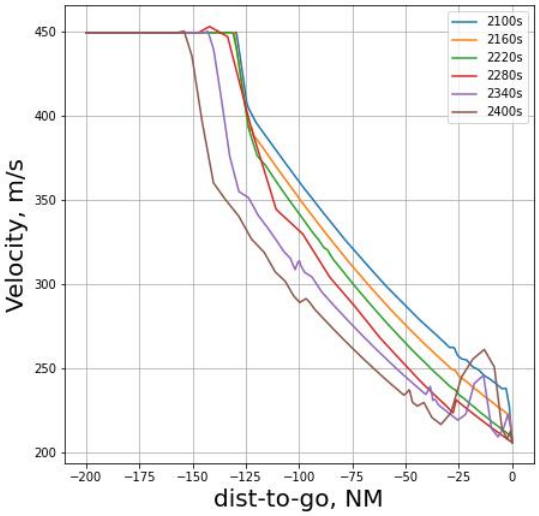

(a) Speed

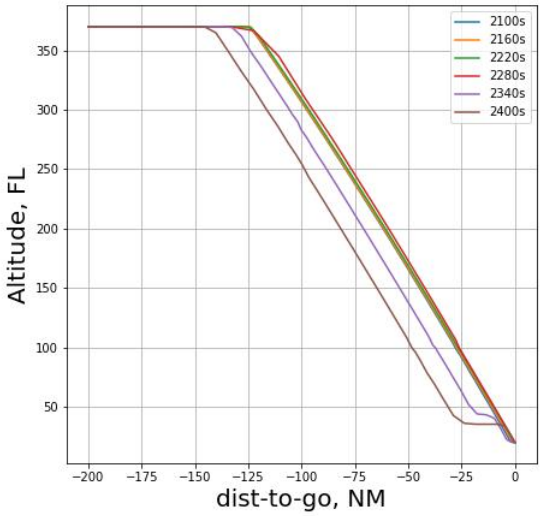

(b) Altitude

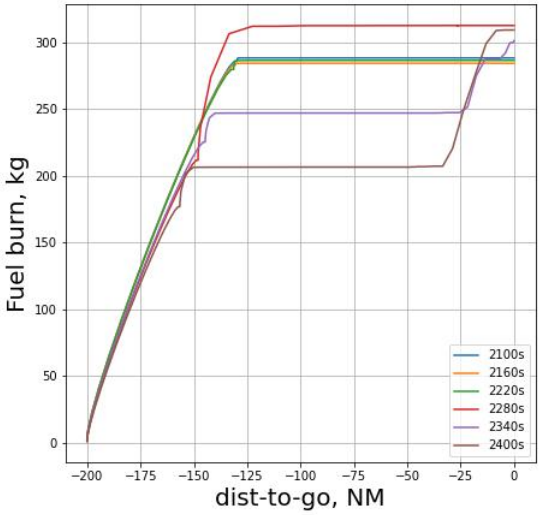

(c) Fuel burn

Figure 2-2: Variation of speed, altitude and fuel burn with distance-to-go, for different values of RTA.

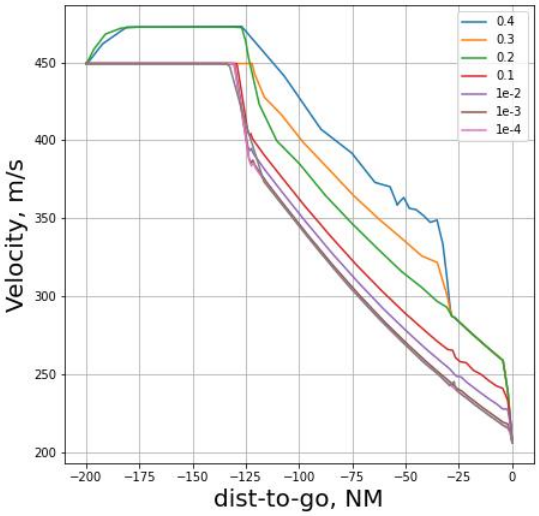

(a) Speed

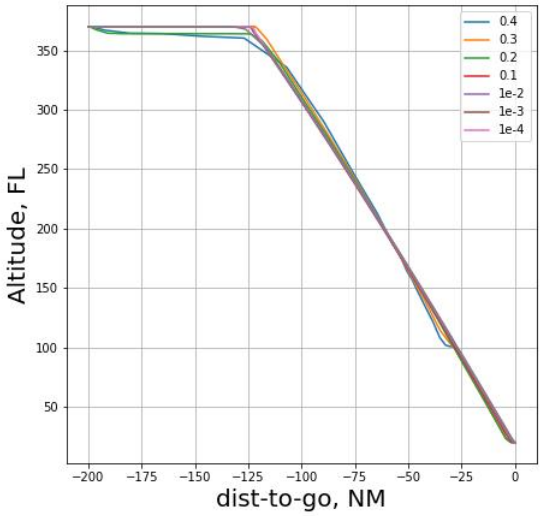

(b) Altitude

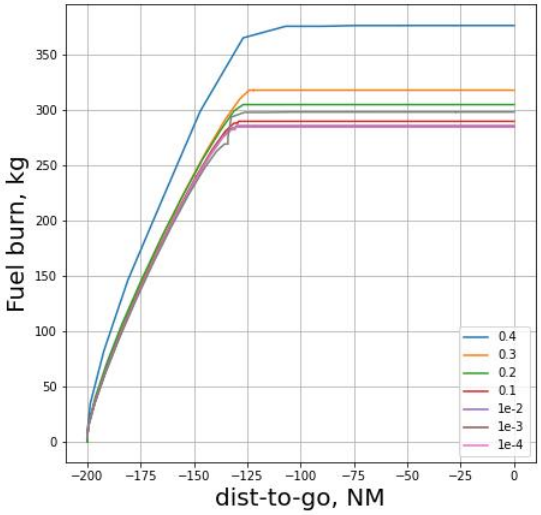

(c) Fuel burn

Figure 2-3: Variation of speed, altitude and fuel burn with distance-to-go, for different values of Cost Index.

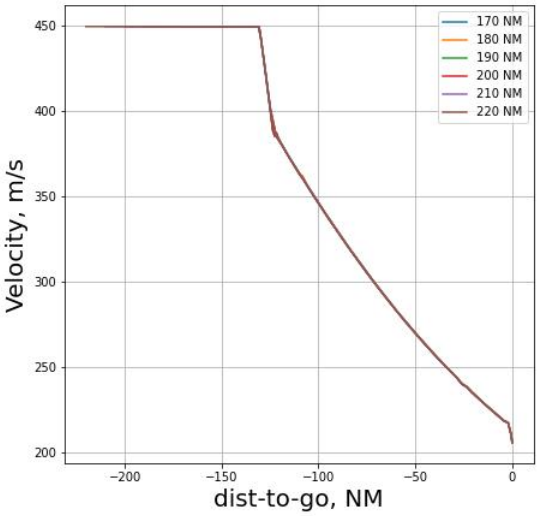

(a) Speed

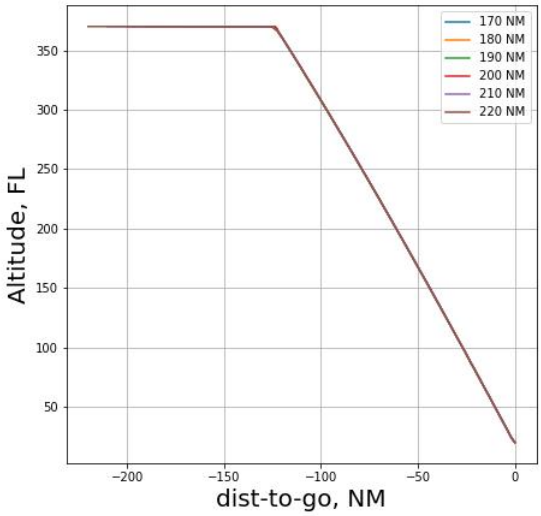

(b) Altitude

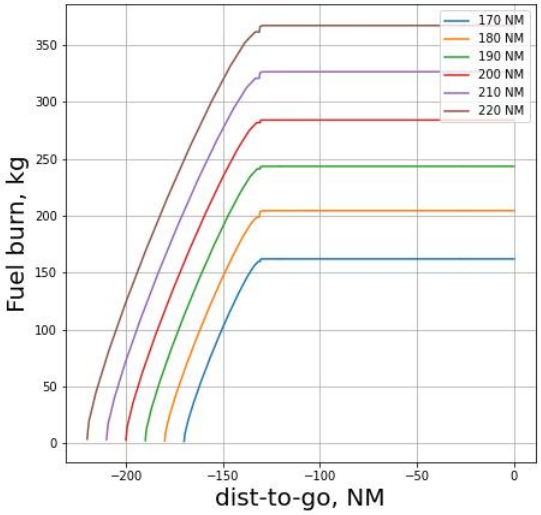

(c) Fuel burn

Figure 2-4: Variation of speed, altitude and fuel burn with distance-to-go, for different values of distance to fix.

Chapter 3

Metering Point Selection

3.1 Trajectory Uncertainty Model

To constantly monitor traffic flows and manage throughput, one or more time constraints, called metering points or RTAs, may be placed at metering fixes along a defined 4D trajectory. During a single metering point operation, the aircraft is required to arrive at a 3D waypoint within a given RTA with a time precision. In practice, when an aircraft assigned an RTA, its FMS initially computes the aircraft's Estimated Time of Arrival (ETA), and if different from the assigned RTA (due to wind or modeling errors), a speed adjustment is made to ensure the ETA matches the RTA. Many commercial FMS are already equipped with an RTA functionality to perform such operations [34]. As mentioned in the introduction, wind error is one of the main sources of uncertainty in an aircraft's trajectory, and is the main subject of consideration in this research. Describing the amount of uncertainty will also require an understanding of the amount of speed correction needed so that the aircraft arrives within a desired tolerance. A few studies have researched speed adjustment policies [57, 109], and one of them [57] is adopted in this project.

Let the uncertainty in an aircraft's trajectory be defined as the difference between the actual x_{act} and predicted trajectories x_{pred}:

$$x = x_{act} - x_{pred} \tag{3.1}$$

If this uncertainty is caused by a wind forecast uncertainty $w(t) = U_{w,act} - U_{w,pred}$, a speed adjustment $s(t)$ needs to be added to the predicted ground speed $V_{pred} = \frac{dx_{pred}}{dt}$ to meet the Required Time of Arrival. This gives the mathematical expression:

$$\frac{dx_{act}}{dt} = V_{pred}(t) + w(t) - s(t) \tag{3.2}$$

Combining 3.1 and 3.2 describes the uncertainty dynamics as::

$$\frac{dx}{dt} = w(t) - s(t), \tag{3.3}$$

The uncertainty solely depends on wind error and speed correction, and is independent of actual aircraft speed. A possible consequence of is that the path deviates from its planned altitude profile being idle thrust. Therefore, it is assumed that a path managed descent is being performed, that is, the speed profile changes while the altitude remains fixed, this is achieved by elevator control of the aircraft when there is a speed correction to maintain its geometric descent. If the speed deviation is too far thrust may be added to compensate. For the purposes of this research, the wind forecast uncertainty $w(t)$ is set to a constant value w_0 for the entire duration of the profile, which is analogous to assuming a worst case wind uncertainty.

The aircraft has to be at a metering fix within a certain time. This time tolerance is translated into distance x_{tol} using the aircraft's speed, constraining $x(t)$ at the RTA waypoint. Without any restrictions, the speed correction strategy $s_{cor}(t)$ is expressed as follows [57, 70]:

$$s_{cor}(t) = \begin{cases} \frac{x(t)}{RTA-t}, & t \leq t_1 \\ s_{cor}\left(t_1\right), & t > t_1 \end{cases} \tag{3.4}$$

$$t_1 = RTA - \frac{x_{tol}}{w_0} \tag{3.5}$$

$$\tag{3.6}$$

The intuition here is that after the aircraft has accumulated uncertainty due to the wind $w(t) = w_0$, a gradient value of $\frac{x(t)-0}{RTA-t}$ has to be subtracted from the actual

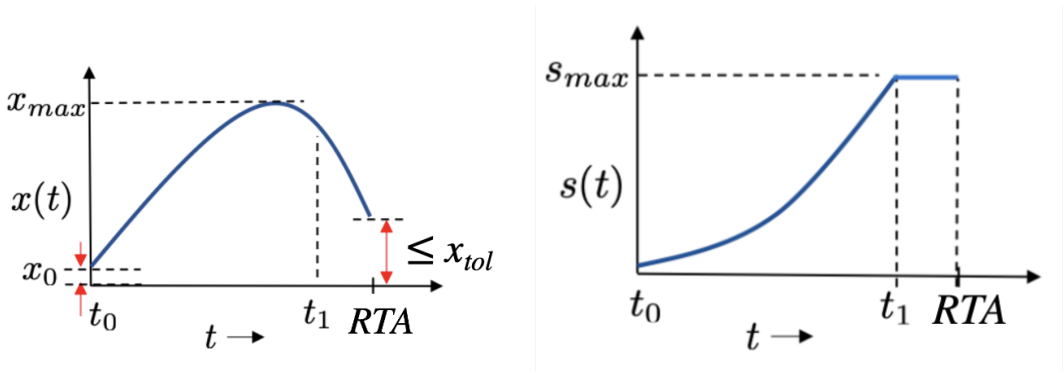

(a) Trajectory deviation $x(t)$ (b) Speed correction $s(t)$

Figure 3-1: Speed correction policy and uncertainty profiles

slope dx/dt in order to drive $x(t)$ to zero. At time t_1, the current speed correction is sufficient to keep the aircraft remain within the desired tolerance for the rest of the operation. The CDA profile has maximum allowable speeds determined as the difference between the airspeed and operational constraints. If the required speed correction $s(t)$ exceeds the maximum allowable speed $s_{max}(t)$ as determined by the available speed window, then it is set to this maximum value.

$$s(t) = \min\left(s_{cor}(t), s_{max}(t)\right) \tag{3.7}$$

It is also certainly possible to re-optimize the CDA trajectory when there are disturbances, but for the sake of simplicity and how well it bounds the values for actual operations [57] the uncertainty is calculated separately. Not only that, but using this analytical model it reduces the amount of complexity when examining a sequence of RTAs [70].

Execution

Typically, there are two ways ATC makes flights conform to scheduled time of arrival (STA): speed change and path stretches. As previously mentioned, speed changes are executed by either elevator control or additional thrust in this model while the geometric descent is managed. Using elevator control to change speed [89] can maintain idle thrust by addition or subtracting the potential term $m\sin(\gamma)$ term in equation

3.8

$$T = D + m\dot{V} + m\,\sin(\gamma) \tag{3.8}$$

The amount of change in flight path angle can be defined as:

$$\gamma = \sin^{-1}\left(\frac{(T_{idle} - D - m\dot{V})}{mg}\right); \gamma_{min} \leq \gamma \leq 0 \tag{3.9}$$

However, this method is limited by the values the track angle is bounded by. In cases when elevator control is not enough, additional thrust or speed brakes will have to be used.

Feasible Parameter Space

Having an available speed window also implies a certain range of possible wind error and initial uncertainty values the aircraft can correct. For a set of initial uncertainty x_0 and wind error w_0 figure 3-2 provides the solution space given a speed window. Values above zero in $x_f - x_{tol}$ indicates that the aircraft is unable to reach within the desired tolerance at the end of the profile.

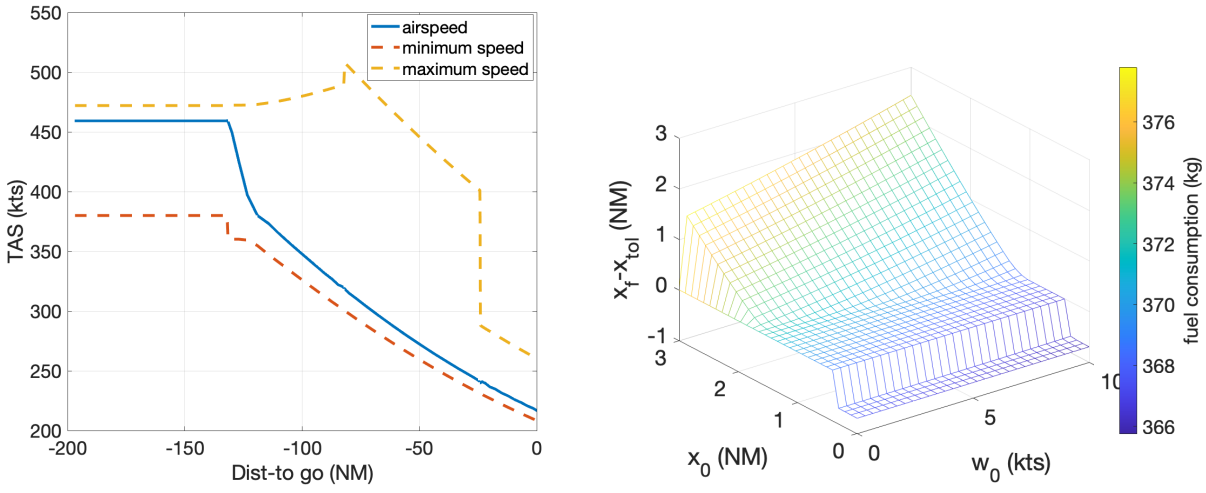

(a) Speed range

(b) Feasible space

Figure 3-2: Feasible solution space given a speed range of values

3.2 Selection of Metering Points

The previous sub-section discussed the method of meeting a path with a single RTA, but multiple intermediate RTAs may also be placed to further assist aircraft flow merging and deconfliction. For a 4D trajectory with a sequence of RTA waypoints, the uncertainty at prior waypoints will affect subsequent ones. The final uncertainty at the preceding waypoint becomes the initial condition for the next, and if not properly managed, can cause future deviations to grow. Furthermore, the distance between consecutive RTA waypoints impacts fuel consumption (because of required speed corrections) and throughput. The optimized CDA profile (Sec. 2) is assumed to be the planned route, with a fixed RTA waypoint at the end of the trajectory(IAF/FAF). Our goal is to optimally locate intermediate waypoints along the CDA profile prior to the final fix, taking into consideration the throughput and fuel consumption.

For the rest of this thesis, locations of the flight with RTA constraints will also be referred to as metering points, waypoints or metering fixes in this section. The connection between subsequent RTA waypoints will also be called RTA links/time links.

3.2.1 Performance Metrics: Throughput and Fuel Burn

In order to formulate an optimization problem to optimally select intermediate RTAs, the relationship between operational parameters such as throughput and fuel consumption is investigated with respect to the flight profile and assigned RTAs.

Throughput

Aircraft throughput is defined as the number of aircraft that can pass through a link (connection between two points on a trajectory) over a period of time while satisfying the minimum separation requirements. It is calculated as per the required time separation between two aircraft passing through a link. The time separation t_{sep} at a flight location is the required separation distance between two aircraft, x_{req}, divided by the ground speed, V_{GS}. To compute this, the true airspeed is corrected

to account for the required speed correction, which makes the realized ground speed $V_{\mathrm{GS}}(t) = V(t) - s(t) + w(t)$. The throughput of a link can then be computed as the inverse of the maximum time separation required in that link.

$$t_{\mathrm{sep}} = \frac{x_{\mathrm{spacing}}(t)}{V_{\mathrm{GS}}(t)} = \frac{2x(t) + x_{\mathrm{req}}}{V(t) + w(t) - s(t)} \tag{3.10}$$

$$P_{\mathrm{link}} = \frac{1}{\max t_{\mathrm{sep}}}, \tag{3.11}$$

where V is the speed obtained from the CDA optimization problem, and x_{req} is the required minimum separation. This minimum required spacing is set to be 3 NM based on terminal-area aircraft operations, while the $x(t)$ and $s(t)$ profiles are derived from the uncertainty calculation in that link ((3.3) (3.7)). The term $2x(t)$ is added to the spacing to account for the maximum position uncertainty of two consecutive aircraft following the same profile. This term is necessary because, even though the desired spacing is achieved at the start and end of a link, spacing infringement could occur in-between. For a given link, it can be inferred from the throughput equation that higher minimum speeds and smaller aircraft spacing will result in a larger throughput. Additionally, the shorter the distance between two consecutive RTA waypoints, the smaller maximum uncertainty $x_{\max}$ of the link, leading to a higher throughput (and vice versa).

Fuel Consumption

The nominal fuel flow equation given in (2.10) and is integrated over the entire operation to obtain the total fuel consumption, $\mathcal{F}$. The speed correction policy $s(t)$ is subtracted from $V(t)$ to obtain the actual true airspeed. This change in speed will affect the amount of generated thrust (3.8) , and ultimately the fuel burn. The fuel consumption of a link that begins at time t_0 and ends at time t_{RTA} is computed as:

$$\mathcal{F} = \int_{t_0}^{t_{\mathrm{RTA}}} \dot{F}_{\mathrm{fuel}}(t) dt \tag{3.12}$$

where $\dot{F}_{\mathrm{fuel}}(t)$ is given by (2.10).

3.2.2 Optimal Location of Intermediate RTA Waypoints

To determine placement of $N-1$ intermediate RTA waypoints, the descent trajectory is divided into N links, each represented by an duration t_i (i.e., the time-difference between the RTAs at the two ends). Each link will have an associated throughput and fuel costs. The objective is to select a set of points that minimizes total fuel burned for the entire trajectory, and maximizes the throughput. This can be represented as the following optimization problem:

$$\text{minimize} \sum_{i=1}^{N} \mathcal{F}_i - \alpha \min P_i \tag{3.13}$$

$$\text{such that} \sum_{i=1}^{N} t_i \leq t_{\text{total}} \tag{3.14}$$

$$P_i \geq D, \; \forall i = 1, \cdots, N \tag{3.15}$$

$$t_{\min} \leq t_i \leq t_{\max} \tag{3.16}$$

where α is the relative weight placed on throughput relative to fuel burn in the objective function, t_i is the duration of link i, D is the demand for the entire CDA operation, P_i is the minimum throughput for link t_{i-1} to t_i, f_i is the corresponding total fuel burn, $t_{\min}$ and $t_{\max}$ are the minimum and maximum allowable values of t_i, and t_{total} is the total flight time to the end of the trajectory.

The number of variables in the optimization problem are specified by the number of RTA waypoints defined during the planned trajectory. For example, a single intermediate RTA waypoint will correspond to two links of length t_1 and t_2: the first from the initial point to an intermediate RTA waypoint, and the second from the intermediate RTA waypoint to the final fix. The time durations t_i must sum to total time given by the planned CDA trajectory, this explains constraint (3.14). The average throughput for each link is also required to be greater than the given demand (3.15), and the intermediate constraints are bounded by the smallest achievable RTA duration (3.16). These values depend on how much speed control authority is available: if the RTA is too small, the speed correction needed will be too high to complete

the operation. The `surrogateopt` tool in MATLAB is used to solve this optimization problem.

Chapter 4

Numerical Results

The concepts introduced in Chapters 2 and 3 are applied to an airport's terminal area in this chapter. First, descent profiles from historical data are compared to generated CDA profiles. Next, the placement of metering points and their impact on fuel burn and throughput is discussed. Finally, the effect of varying variables like wind error magnitude and number of metering points is explored.

4.1 Case Study: Hartsfield-Jackson Atlanta International Airport

In this section, chart information for a Standard Arrival Route (STAR) approach procedure is used to design phase constraints for the CDA optimization problem. The STAR arrival route serves as the transition between the en-route phase of the flight and approach just before landing, therefore it is appropriate for this application. Being America's busiest airport, Hartsfield-Jackson Atlanta International Airport (ATL) is selected for this problem. As previously noted, aircrafts undergo step-down approaches (SDA) that contain multiple level offs at lower altitudes to manage throughput and deconflict trajectories. Therefore, to highlight the difference between generated CDA profiles and regular arrivals at this airport, sample flight trajectories were obtained from FlightAware.com [110]. ADS-B data of Boeing 752

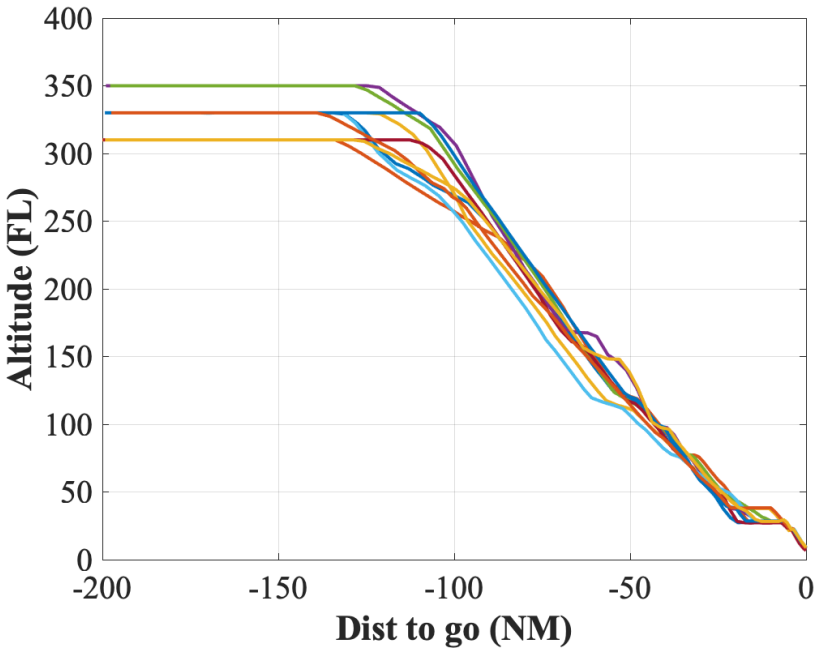

Figure 4-1: SDA Flight Trajectories at ATL

and 737 flights taking place between 13th of April to 21st of April 2022 at ATL were used as the required SDA trajectories (Fig. 4-1).

4.1.1 Flight Profile Generation

The selected STAR approach is the JJEDI TWO arrival procedure shown in Fig. 4-2. After cruising, the aircraft completes the LARZZ transition before proceeding to ILS 27L runway (see Figs. 4-3 and 4-4). Altitude, distance, and speed constraints to solve the optimization problem in 2.11 are obtained from these diagrams and summarized in Table 4.1. These path restrictions are encoded into the problem in form of path, event and algebraic constraints. In a nutshell, the entire CDA profile is divided into 8 phases from cruise to the last two fixes: Initial approach fix SYLAA at or above (AOA) 7000ft and final approach fix DEPOT AOA 2800 ft. An additional waypoint was added between cruise and LARZZ to define the Top of Descent location. In addition to the limitations by the charts, cruise altitude h_0 is determined by the SDA flight it will be compared with and total distance to go s_0 is set to 200NM. Finally, speed boundaries between waypoints are defined such that their values are

Waypoint	Altitude	Speed
LAIRI		
LARZZ	A0A FL240	
DTSTR	AOA 14000	AT 280KT
WOKIE	AOA 11000	AT 250KT
JJEDI	AOA 10000	AT 250KT
DAFII	AT 8000	
SYLAA	AOA 6000	
DEPOT	AOA 2800	

Table 4.1: STAR Waypoints

Phase	Description	Path Constraints	Initial and Final Conditions
c	Cruise to ToD	$M_{\min} \leq M \leq M_{MO}$ $h = h_{cruise}, \gamma = 0^\circ$	$s_I = -200$NM
d_1	ToD to LARZZ	$M_{\min} \leq M \leq M_{MO}$	$h_F \geq$ FL240, $s_F = -105$NM
d_2	LARZZ to DTSTR	280kt $\leq V_{CAS} \leq V_{MO}$	$h_F \geq 14000$ft, $s_F = -59$NM $V_{CAS,F} = 280$kt
d_3	DTSTR to WOKIE	230kt $\leq V_{CAS} \leq V_{MO}$	$h_F \geq 11000$ft, $s_F = -44$NM $V_{CAS,F} = 250$kt
d_4	WOKIE to JJEDI	210kt $\leq V_{CAS} \leq 250$kt	$h_F \geq 10000$ft, $s_F = -40$NM $V_{CAS,F} = 250$kt
d_5	JJEDI to DAFII	180kt $\leq V_{CAS} \leq 250$kt	$h_F = 8000$ft, $s_F = -31$NM
d_6	DAFII to SYLAA	180kt $\leq V_{CAS} \leq 210$kt	$h_F \geq 7000$ft, , $s_F = -19$NM $V_{CAS,F} = 180$kt
d_7	SYLAA to DEPOT	180kt $\leq V_{CAS} \leq 210$kt	$h_F \geq 2800$ft, , $s_F = -3.5$NM $V_{CAS,F} = 180$kt

Table 4.2: Path Constraints

reasonable and control input bounds are the same as Table 2.3. Speed and altitude constraints from the STAR procedure and runway are listed in Table 4.1 while all phase constraints are in Table 4.2.

The CDA profiles are optimized with a constant constant 2 kts value . Comparisons to the conventional SDA trajectories are presented in Fig. 4-5. First and foremost, it is noticeable that the aircraft spends longer time at higher altitudes such as cruise for the CDA profiles versus SDA. The level-off initially located at approximately 3000 ft has now been elevated to 8000 ft, moving the speed profile to a more optimal form. Although the aircraft flies longer at higher altitudes, a level off is still

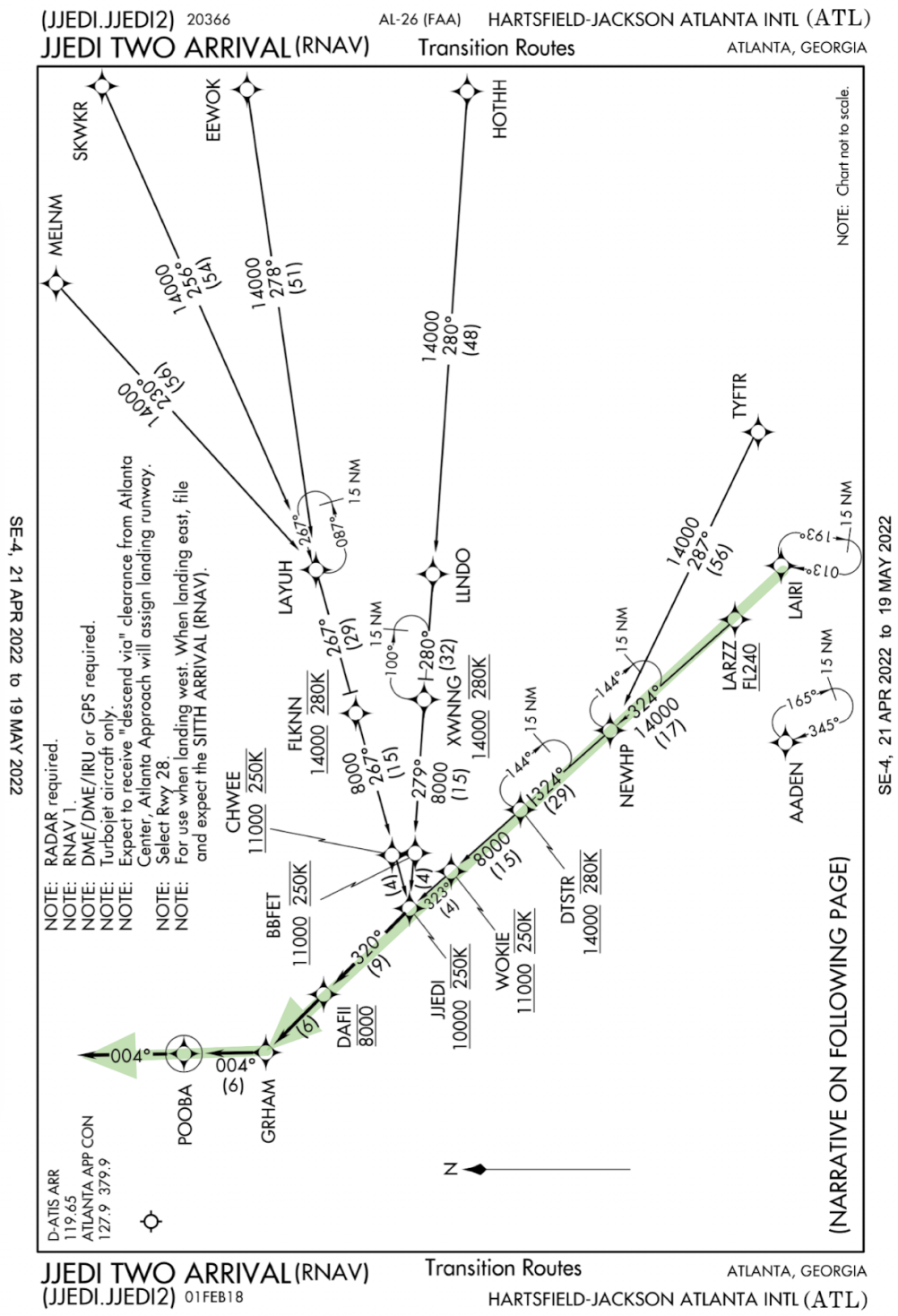

Figure 4-2: JJEDI STAR Procedure (highlighted portion is the route to be considered)

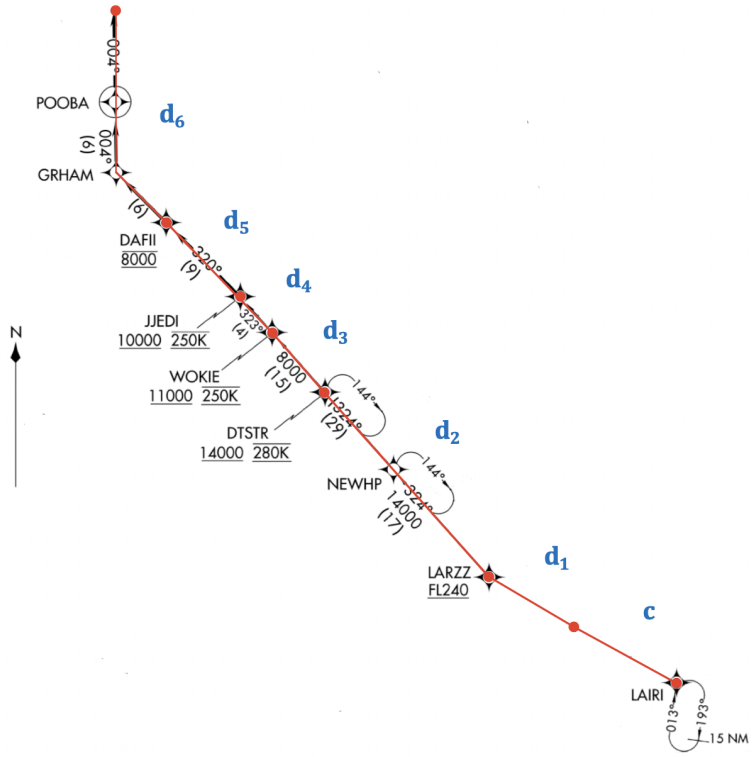

Figure 4-3: JJEDI STAR Procedure

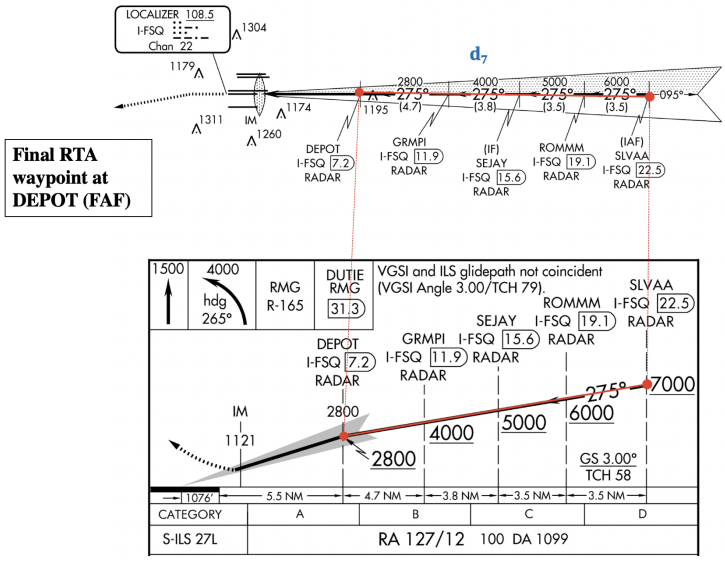

Figure 4-4: Instrument Landing System (ILS) procedure to the runway

experienced at 8000 ft due to meeting the STAR procedure requirement of the aircraft to be AT 8000ft at that waypoint.

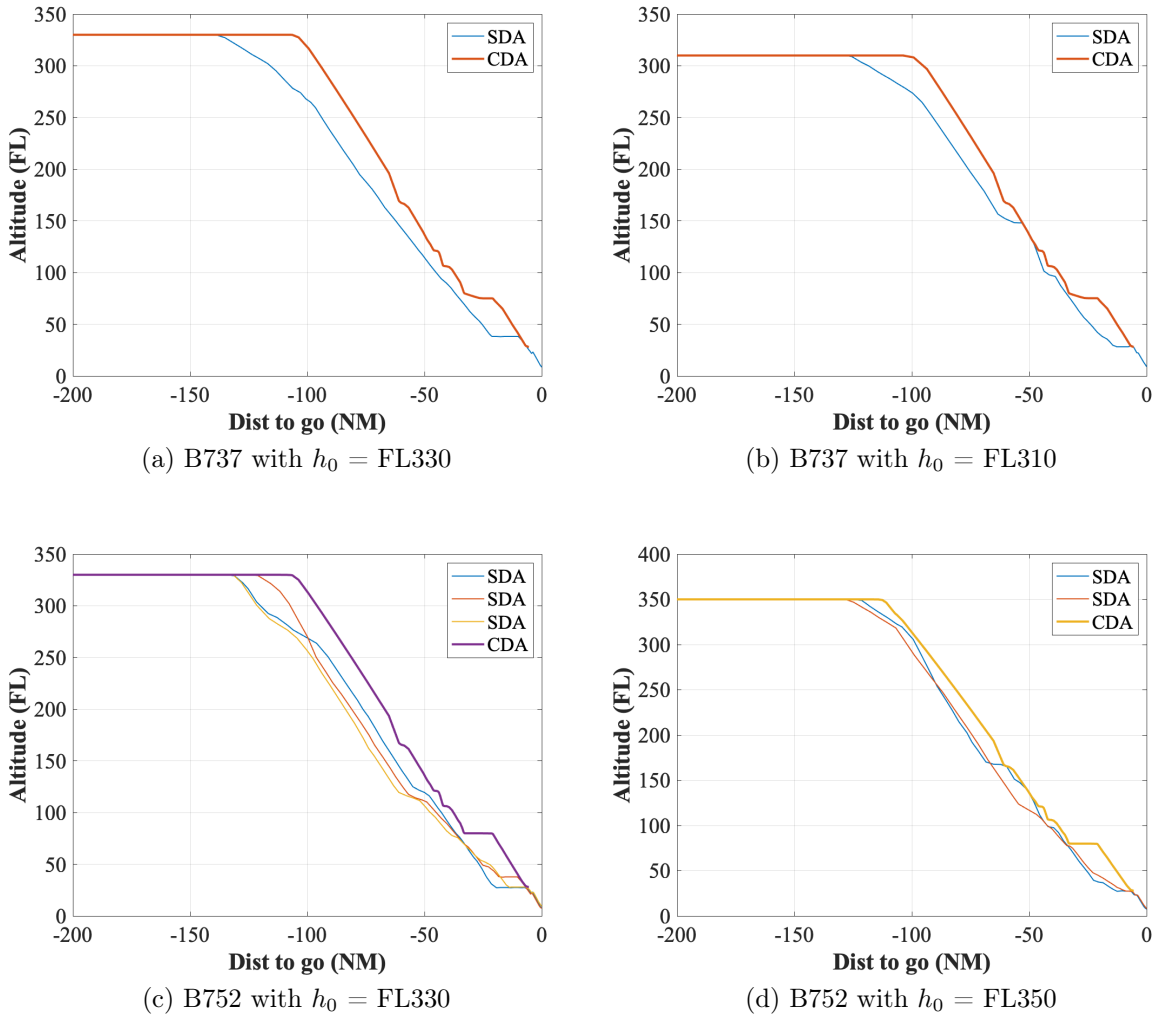

(a) B737 with h_0 = FL330

(b) B737 with h_0 = FL310

(c) B752 with h_0 = FL330

(d) B752 with h_0 = FL350

Figure 4-5: CDA vs Conventional FLight at various altitudes

4.2 Metering Point Selection

4.2.1 Single Metering Point

The factors affecting fuel burn can be investigated over a CDA flight which has a single RTA located at the end of its trajectory. A seen in fig. 4-6b, most of the accumulation in fuel burn uncertainty happens later in the flight, this is also where the available speed correction window is smaller, and the noticeable jump in fuel uncertainty located -31 NM from the end can be attributed to the level-off at 8000ft. For similar reasons the throughput is lowest towards the end of the trajectory. If a single RTA was placed in this case, the throughput will be the lowest value 35 aircraft/hr. The next sub-section explores how placing intermediate RTA points can increase this throughput and what change in fuel consumption is required.

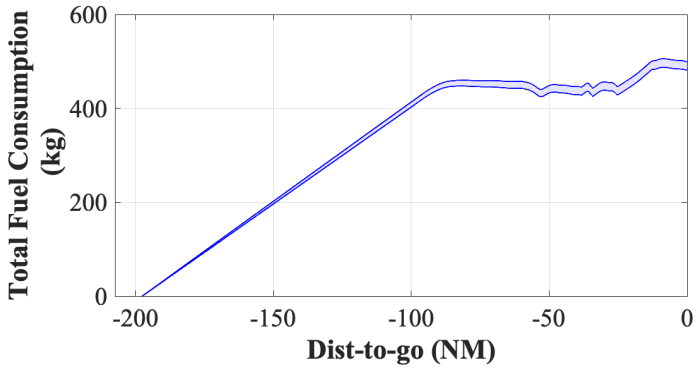

(a) Fuel Flow Rate

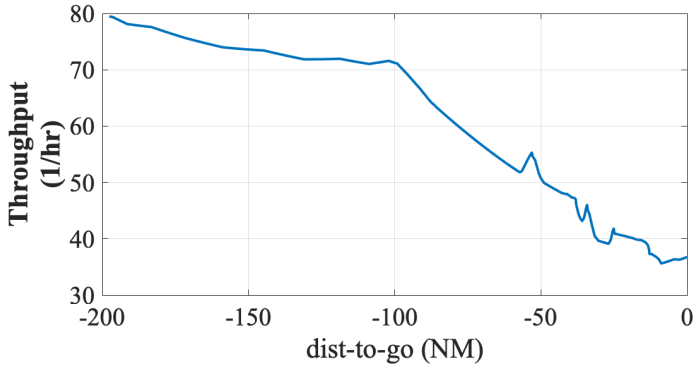

(b) Fuel consumption

Figure 4-6: Fuel burn rate and cumulative fuel consumption along the trajectory, given a single RTA waypoint located at DEPOT.

4.2.2 Multiple Metering Points

To understand the effect of adding intermediate RTA waypoints, the number of such points is varied, and the optimization problem (3.13)-(3.16) is solved. The scaling factor α between the two costs is varied to increase or decrease the weight placed on throughput, and can be adjusted based on user preferences. A higher value of α reflects a scenario where more throughput is needed at the expense of some fuel expenditure; the amount of such additional fuel is what is being explored here. Fig. 4-7 shows an example of the optimal location of two intermediate RTA waypoints along a CDA profile (i.e., $N = 3$).

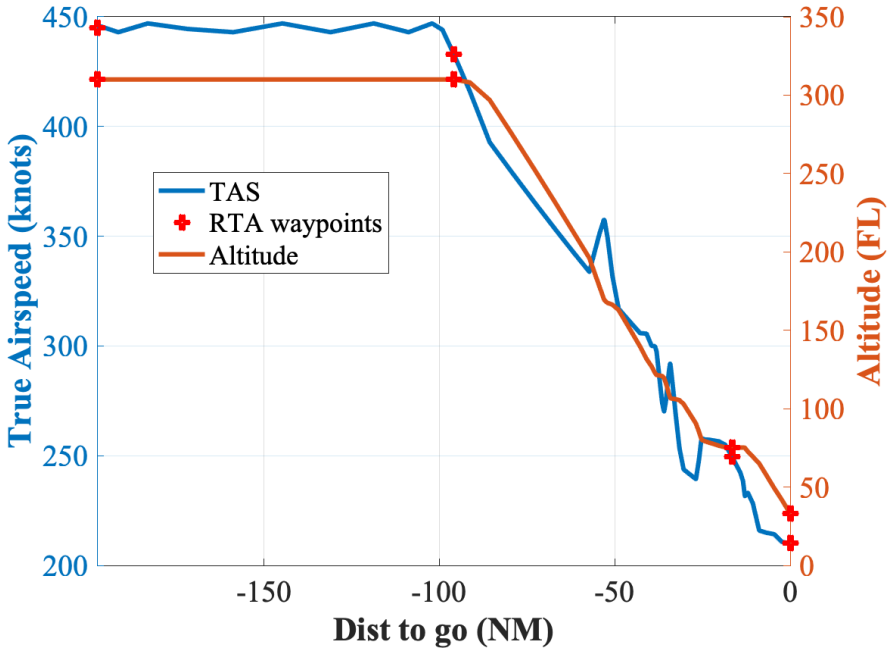

Figure 4-7: Optimal intermediate RTA waypoint locations for $N = 3$.

Number of Metering points

Comparisons are made with respect to the to the baseline trajectories ($N = 1$) which uses single RTA waypoint (placed at the end) for the entire descent profile. The baseline trajectories are the CDA profiles with a single metering RTA. Fig. 4-8 shows how the total fuel burn and throughput change with number of RTA waypoints for generated CDA profile in Fig. 3-2a, for both maximum and minimum speed profiles

caused by negative and positive wind errors (the left and right points, respectively). The analysis shows that higher throughput can indeed be achieved by increasing the number of points, but is accompanied by an increase in fuel consumption (especially when the wind errors are negative). This is to be expected: as the number of RTA waypoints increases, the aircraft makes more speed corrections to meet the RTAs, incurring fuel costs. However, more RTA waypoints yields better predictability and increased throughput. To drive this point home, analysis can be completed for the multiple generated CDA profiles of B737 and B752 (Fig. 4-5) in Fig. 4-9. The both axes are scaled to place values of two different aircrafts that have different fuel consumption and throughput properties in the same graph. In general, similar results are seen as a positive correlation is observed for negative wind errors and vice versa.

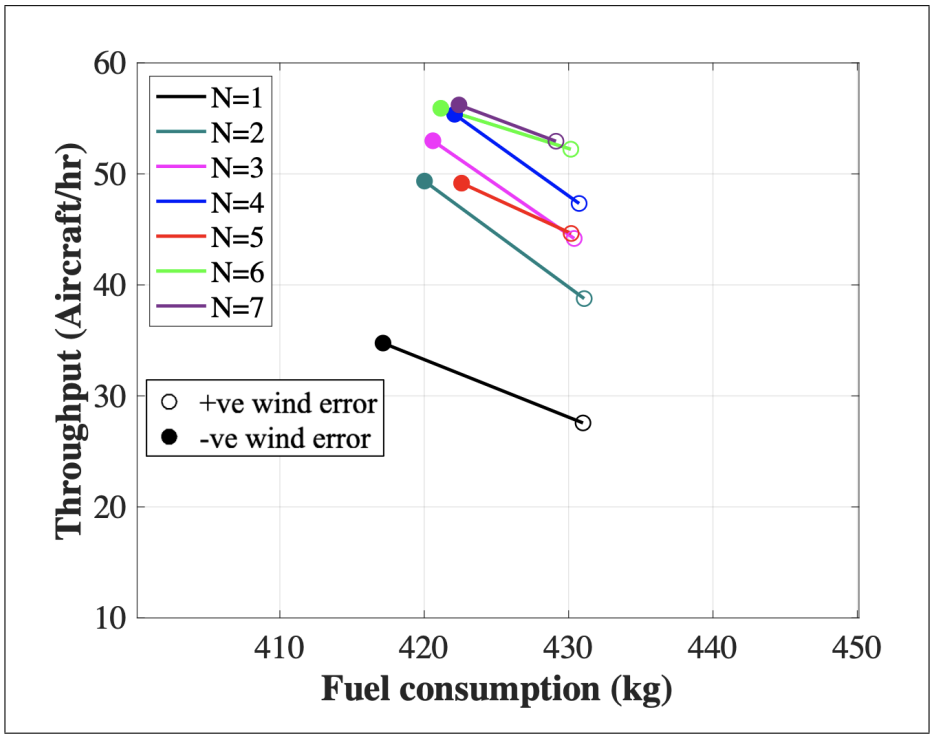

Figure 4-8: Throughput vs. fuel consumption, for varying number of RTA waypoints, N. The solid markers denote negative wind errors, and the unfilled markers denote positive wind errors. $\alpha = 10$.

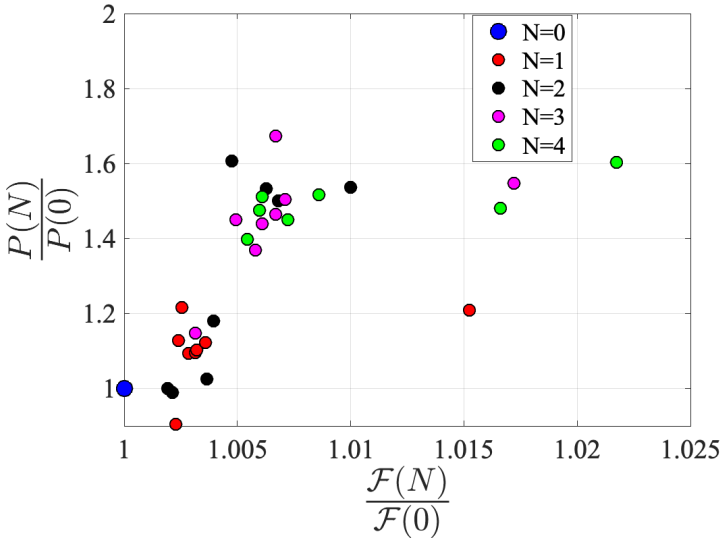

(a) Negative wind errors

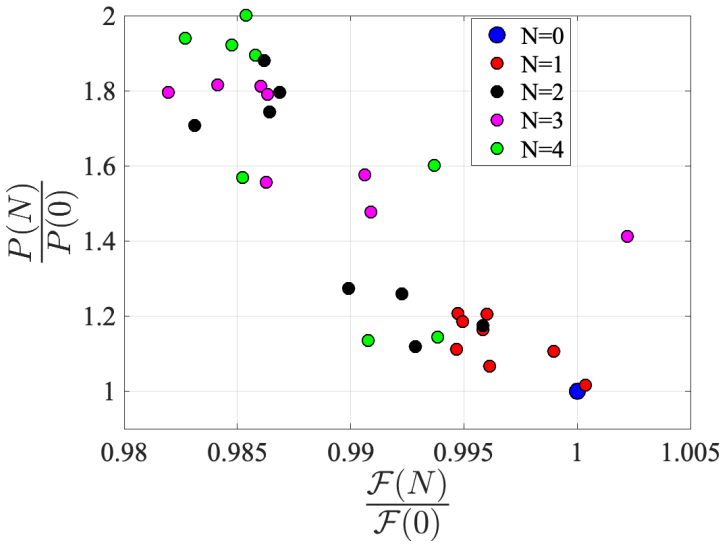

(b) Positive wind errors

Figure 4-9: Throughput vs. fuel consumption, for varying number of RTA waypoints, N.

Growth in Uncertainty

The reduction in difference between the minimum and maximum velocity parameters also reflects the fact that predictability is improved with higher N. This is also seen in Fig. 4-10, where the final deviation of the aircraft trajectory decreases as the number of RTA waypoints increases.

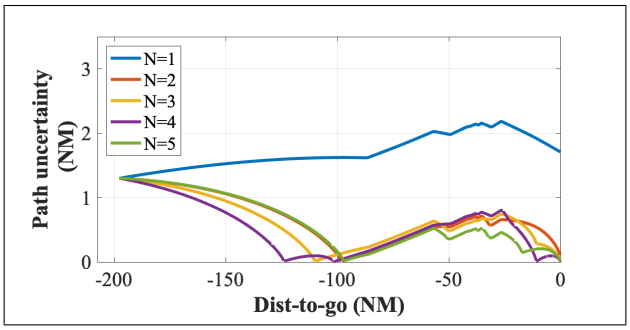

Figure 4-10: Trajectory spatial (path) uncertainty along the descent profile, for varying number of RTA waypoints, N.

4.3 Variations in Parameters

4.3.1 Maximum Magnitude of Wind Error

The relationship between the fuel burn and throughput will be affected by the wind forecast error magnitude as demonstrated in Fig. 4-11. In general, a higher absolute wind error will cause an increase in fuel consumption, as the aircraft needs more speed to compensate.

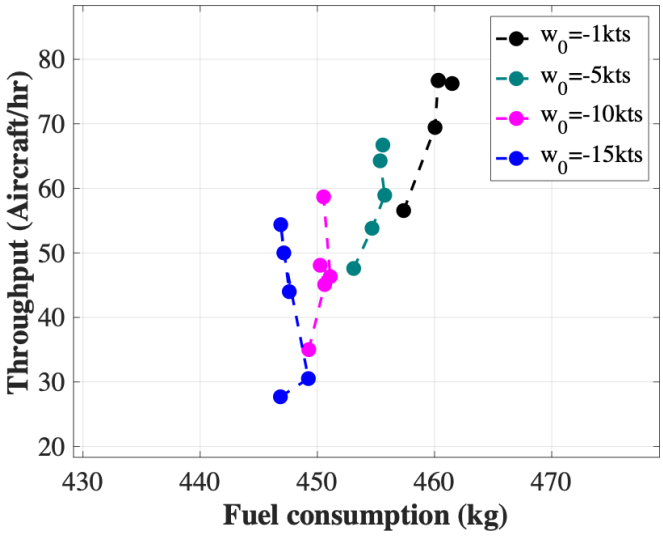

Figure 4-11: Wind error magnitude variation

Chapter 5

Conclusion and Future Work

This thesis presented an approach for trajectory specification, i.e, to optimally locate intermediate waypoints with associated time-constraints (called RTA waypoints) along a Continuous Descent Approach (CDA) profile, in order to support high throughput. Doing so allows one to leverage the increased predictability of Trajectory-Based Operations (TBO) to overcome the potential loss in throughput of CDA operations due to increased uncertainty. Consequently, this method is a step toward enabling CDAs in high-density terminal-areas. However, while adding intermediate RTA waypoints can increase throughput and predictability, it is at the expense of additional fuel costs in the presence of winds.

This approach was divided into two problems, first designing a CDA procedure, then creating waypoints along the generated profile. A multi-phase optimization strategy was formulated to design a CDA profile that minimized fuel consumption and time. Aircraft dynamics and speed, altitude and distance requirements from a given arrival procedure were encoded as constraints in the problem. The terminal procedure consisted of 8 phases based on a LARZZ transition of JJEDI2 STAR procedure and ILS 27L runway at ATL airport. When compared to regular step-down descents, the generated CDA profiles flew at higher altitudes for longer. Next, the metering points were selected based on another optimization problem that minimized fuel consumption and throughput. These two parameters were analyzed with respected to number of waypoints specified, as well as other variables like wind error

magnitude. Results showed that throughput can by improved by as much as 70%, while incurring additional fuel costs of up to 2% per flight.

While this thesis focused on CDAs, similar analysis may be conducted for conventional step-down approaches. Furthermore, the uncertainty model used was an open-loop; it is worth considering how closed-loop 4D trajectories could affect the results. There were also multiple simplifications that could be relaxed. The aircraft dynamics consisted of 3 degrees-of-freedom (DOF) (altitude, longitudinal distance and track angle), further evaluations can be made for the entire 6-DOF problem. Finally, the incorporation of more sophisticated wind models or other sources of uncertainty is an important direction for further investigation. Future work will also include using other forms of robust control strategies. This may affect the amount of fuel burn if less speed control is used. Finally, the investigation of other sources of uncertainty besides wind errors is an interesting direction for future research.

Bibliography

[1] A Gittens, S Hocquard, A de Juniac, F Liu, and E Fanning. Aviation benefits report. In *Convention on International Civil Aviation*, volume 76, 2019.

[2] ICAO. Long-term traffic forecasts, 2019.

[3] Patricia Hu, Rolf R Schmitt, Julianne Schwarzer, William H Moore, et al. Transportation statistics annual report 2021. 2021.

[4] SESAR Joint Undertaking. European atm master plan–digitalising europes's aviation infrasturcture. *Sesar Joint Undertaking*, 2020.

[5] M Gregorova. Eurocontrol long-term forecast: Flight movements 2010-2030, 2010.

[6] Statistics EUROCONTROL. European aviation in 2040—challenges of growth, 2018.

[7] IATA (International Air Transport Association). Industry statistics. fact sheet october 2021. 2021.

[8] IATA. Fuel fact sheet, 2021.

[9] ICAO. Destination green: the next chapter, 2019.

[10] Michael Gill. Aviation benefits beyond borders. *Air Transport Action Group (ATAG)*, 1(1), 2016.

[11] Stefan Gössling and Andreas Humpe. The global scale, distribution and growth of aviation: Implications for climate change. *Global Environmental Change*, 65:102194, November 2020.

[12] Jeff Overton. The growth in greenhouse gas emissions from commercial aviation. *EESI, url: https://www. eesi. org/papers/view/fact-sheet-the-growth-ingreenhouse-gas-emissions-from-commercial-aviation [accessed: 2021-04-23]*, 2019.

[13] D.S. Lee, D.W. Fahey, A. Skowron, M.R. Allen, U. Burkhardt, Q. Chen, S.J. Doherty, S. Freeman, P.M. Forster, J. Fuglestvedt, A. Gettelman, R.R. De León, L.L. Lim, M.T. Lund, R.J. Millar, B. Owen, J.E. Penner, G. Pitari, M.J.

Prather, R. Sausen, and L.J. Wilcox. The contribution of global aviation to anthropogenic climate forcing for 2000 to 2018. *Atmospheric Environment*, 244, January 2021.

[14] NextGen Integration and Implementation Office. Nextgen implementation plan, 2018.

[15] Jesper Bronsvoort and Greg McDonald. Concept of operations for ATM by managing uncertainty through multiple metering points. In *Air Transport and Operations Symposium 2012*, 2012.

[16] Asei Tezuka. 4D trajectory based operation in high density terminal control area considering the uncertainty of weather forecast data. In *Proceedings of the 29th Congress of the International Council of the Aeronautical Sciences*, 2014.

[17] *Continuous descent operations (CDO) manual.* Number 9931-AN/476 in Doc [Englische Ausgabe]. International Civil Aviation Organization, Montréal, Quebec, 1. ed edition, 2010.

[18] ICAO Doc et al. Global air navigation plan. 2016.

[19] Shih-Yih Young and Kristen Jerome. Optimal profile descent with 4-D trajectory. In *2013 Integrated Communications, Navigation and Surveillance Conference (ICNS)*, Herndon, VA, April 2013. IEEE.

[20] EUROCONTROL. Continuous descent: A guide to implementing continuous descent, 2011.

[21] J.-P. Clarke, J. Brooks, G. Nagle, A. Scacchioli, W. White, and S. R. Liu. Optimized Profile Descent Arrivals at Los Angeles International Airport. *Journal of Aircraft*, 50(2):360–369, March 2013.

[22] F.J.M. Wubben and Joris Busink. Environmental benefits of continuous descent approaches at Schiphol airport compared with conventional approach procedures. 2000.

[23] Kwok-On Tong, Anthony Warren, and John Brown. Continuous Descent Approach Procedure Development for Noise Abatement Tests at Louisville International Airport, KY. In *AIAA's 3rd Annual Aviation Technology, Integration, and Operations (ATIO) Forum*, Denver, Colorado, November 2003. American Institute of Aeronautics and Astronautics.

[24] Jan Stibor and Anders Nyberg. Implementation of continuous descent approaches at Stockholm Arlanda airport, Sweden. In *2009 IEEE/AIAA 28th Digital Avionics Systems Conference*, Orlando, FL, USA, October 2009. IEEE.

[25] I. Wilson and F. Hafner. Benefit Assessment of Using Continuous Descent Approaches at Atlanta. In *24th Digital Avionics Systems Conference*, volume 1, Washington, DC, USA, 2005. IEEE.

[26] S. Alam, M. H. Nguyen, H. A. Abbass, Chris Lokan, M. Ellejmi, and S. Kirby. Multi-Aircraft Dynamic Continuous Descent Approach Methodology for Low-Noise and Emission Guidance. *Journal of Aircraft*, 48(4):1225–1237, July 2011.

[27] Kevin R. Sprong, Kathryn A. Klein, Camille Shiotsuki, James Arrighi, and Sandy Liu. Analysis of AIRE Continuous Descent Arrival operations at Atlanta and Miami. In *2008 IEEE/AIAA 27th Digital Avionics Systems Conference*, St. Paul, MN, USA, October 2008. IEEE.

[28] John Robinson III and Maryam Kamgarpour. Benefits of continuous descent operations in high-density terminal airspace considering scheduling constraints. In *10th AIAA aviation technology, integration, and operations (ATIO) conference*, 2010.

[29] Doris Novak, Antonio Ratković, et al. Operational Aspects of Vertical Navigation during the Approach Phase of Flight: CDA vs. Conventional Step-Down Approach. *Tehnički vjesnik*, 27(2):346–352, 2020.

[30] Li Jin, Yi Cao, and Dengfeng Sun. Investigation of Potential Fuel Savings Due to Continuous-Descent Approach. *Journal of Aircraft*, 50(3):807–816, May 2013.

[31] Enis T. Turgut, Oznur Usanmaz, Mustafa Cavcar, Tuncay Dogeroglu, and Kadir Armutlu. Effects of Descent Flight-Path Angle on Fuel Consumption of Commercial Aircraft. *Journal of Aircraft*, 56(1):313–323, January 2019.

[32] Joel Klooster, Keith Wichman, and Okko Bleeker. 4D Trajectory and Time-of-Arrival Control to Enable Continuous Descent Arrivals. In *AIAA Guidance, Navigation and Control Conference and Exhibit*, Honolulu, Hawaii, August 2008. American Institute of Aeronautics and Astronautics.

[33] Priyank Pradeep and Peng Wei. Predictability, variability and operational feasibility aspect of CDA. In *2017 IEEE Aerospace Conference*, Big Sky, MT, USA, March 2017. IEEE.

[34] Priyank Pradeep. Evaluation of vertical profiles to design continuous descent approach procedure. Master's thesis, Purdue University, 2013.

[35] Daichi Toratani, Navinda Kithmal Wickramasinghe, and Hiroko Hirabayashi. Simulation techniques for arrival procedure design in continuous descent operation. In *2018 Winter Simulation Conference (WSC)*, Gothenburg, Sweden, December 2018. IEEE.

[36] Liling Ren and John-Paul B. Clarke. Flight-Test Evaluation of the Tool for Analysis of Separation and Throughput. *Journal of Aircraft*, 45(1):323–332, January 2008.

[37] Paul Mark Alexander De Jong. Continuous descent operations using energy principles. 2014.

[38] Kwok-On Tong, Ewald G Schoemig, Danial A Boyle, Julien Scharl, and Aslaug Haraldsdottir. Descent profile options for continuous descent arrival procedures within 3d path concept. In *2007 IEEE/AIAA 26th Digital Avionics Systems Conference*, Dallas, TX, USA, October 2007. IEEE.

[39] Ramon Dalmau and Xavier Prats. Controlled time of arrival windows for already initiated energy-neutral continuous descent operations. *Transportation Research Part C: Emerging Technologies*, 85:334–347, 2017.

[40] Noburu Takeichi and Daigo Inami. Arrival-Time Controllability of Tailored Arrival Subjected to Flight-Path Constraints. *Journal of Aircraft*, 47(6):2021–2029, November 2010.

[41] Ramon Dalmau Codina and Xavier Prats Menéndez. Assessment of the feasible CTA windows for efficient spacing with energy-neutral CDO. In *Proceedings of the 7th International Conference on Research in Air Transportation*, 2016.

[42] Michael R. C. Jackson. CDA with RTA in a mixed environment. In *2009 IEEE/AIAA 28th Digital Avionics Systems Conference*, Orlando, FL, USA, October 2009. IEEE.

[43] Ramon Dalmau, Justinas Alenka, and Xavier Prats. Combining the assignment of pre-defined routes and RTAs to sequence and merge arrival traffic. In *17th AIAA Aviation Technology, Integration, and Operations Conference*, Denver, Colorado, June 2017. American Institute of Aeronautics and Astronautics.

[44] Emad A. Alharbi, Layek L. Abdel-Malek, R. John Milne, and Arwa M. Wali. Analytical Model for Enhancing the Adoptability of Continuous Descent Approach at Airports. *Applied Sciences*, 12(3):1506, January 2022.

[45] Gabriele Enea and Marco Porretta. A comparison of 4D-trajectory operations envisioned for NextGen and SESAR, some preliminary findings. In *28th Congress of the International Council of the aeronautical sciences*, volume 5. Optimage Ltd. Edinburgh, UK, 2012.

[46] Zahra Khan, Husni Idris, Robert Vivona, Sharon Woods, and Richard Lanier. Ground Automation Impact on Enabling Continuous Descent in High Density Operations. In *9th AIAA Aviation Technology, Integration, and Operations Conference (ATIO)*, Hilton Head, South Carolina, September 2009. American Institute of Aeronautics and Astronautics.

[47] Javier Lopez-Leones, Miguel A. Vilaplana, Eduardo Gallo, Francisco A. Navarro, and Carlos Querejeta. The Aircraft Intent Description Language: A key enabler for air-ground synchronization in Trajectory-Based Operations. In *2007 IEEE/AIAA 26th Digital Avionics Systems Conference*, Dallas, TX, USA, October 2007. IEEE.

[48] Tasos Nikoleris and Mark Hansen. Queueing Models for Trajectory-Based Aircraft Operations. *Transportation Science*, 46(4):501–511, November 2012.

[49] Bruno Favennec, Eric Hoffman, Aymeric Trzmiel, François Vergne, and Karim Zeghal. The Point Merge Arrival Flow Integration Technique: Towards More Complex Environments and Advanced Continuous Descent. In *9th AIAA Aviation Technology, Integration, and Operations Conference (ATIO)*, Hilton Head, South Carolina, September 2009. American Institute of Aeronautics and Astronautics.

[50] Jose Miguel Canino Rodriguez, Luis Gomez Deniz, Jesus Garcia Herrero, Juan Besada Portas, and Jose Ramon Casar Corredera. A 4D trajectory negotiation protocol for Arrival and Approach sequencing. In *2008 Integrated Communications, Navigation and Surveillance Conference*, Bethesda, MD, USA, May 2008. IEEE.

[51] Yi Cao, Tatsuya Kotegawa, Joseph Post, D Sun, and D DeLaurentis. Evaluation of continuous descent approach as a standard terminal airspace operation. In *9th USA/Europe Air Traffic Management R&D Seminar*. Federal Aviation Administration and EUROCONTROL Berlin, 2011.

[52] Thomas Prevot, Vernol Battiste, Everett Palmer, and Stephen Shelden. Air Traffic Concept Utilizing 4D Trajectories and Airborne Separation Assistance. In *AIAA Guidance, Navigation, and Control Conference and Exhibit*, Austin, Texas, August 2003. American Institute of Aeronautics and Astronautics.

[53] Yang Zhang and Feifei Chen. A Methodology for 4D Trajectory Optimization of Arrival Aircraft in Trajectory Based Operation. In *2018 13th World Congress on Intelligent Control and Automation (WCICA)*, Changsha, China, July 2018. IEEE.

[54] Daichi Toratani. Application of merging optimization to an arrival manager algorithm considering trajectory-based operations. *Transportation Research Part C: Emerging Technologies*, 109:40–59, December 2019.

[55] Daichi Toratani. Merging Optimization Method with Runway Allocation Optimization maximizing Runway Capacity. In *AIAA Scitech 2019 Forum*, San Diego, California, January 2019. American Institute of Aeronautics and Astronautics.

[56] Sally C. Johnson. Characterization of Metering, Merging and Spacing Requirements for Future Trajectory-Based Operations. In *17th AIAA Aviation Technology, Integration, and Operations Conference*, Denver, Colorado, June 2017. American Institute of Aeronautics and Astronautics.

[57] David De Smedt, Jesper Bronsvoort, and Greg McDonald. Model for longitudinal uncertainty during controlled time of arrival operations. In *10th*

USA/Europe Air Traffic Management Research and Development Seminar, 2015.

[58] Lisha Ye, Li Cao, Shuli Gong, and Jiyun Lu. Optimization of Speed Profile with RTA Constraints under Wind Uncertainty. *Mathematical Problems in Engineering*, 2020, May 2020.

[59] Manuel Soler, Alberto Olivares, and Ernesto Staffetti. Multiphase Optimal Control Framework for Commercial Aircraft Four-Dimensional Flight-Planning Problems. *Journal of Aircraft*, 52(1):274–286, January 2015.

[60] Daniel González-Arribas, Manuel Soler, and Manuel Sanjurjo-Rivo. Robust Aircraft Trajectory Planning Under Wind Uncertainty Using Optimal Control. *Journal of Guidance, Control, and Dynamics*, 41(3):673–688, March 2018.

[61] Antonio Franco, Damián Rivas, and Alfonso Valenzuela. Probabilistic aircraft trajectory prediction in cruise flight considering ensemble wind forecasts. *Aerospace Science and Technology*, 82-83:350–362, November 2018.

[62] David De Smedt and Gerhard Berz. Study of the required time of arrival function of current FMS in an ATM context. In *2007 IEEE/AIAA 26th Digital Avionics Systems Conference*, Dallas, TX, USA, October 2007. IEEE.

[63] Joel K Klooster, Ana Del Amo, and Patrick Manzi. Controlled Time-of-Arrival Flight Trials. In *8th USA/Europe ATM Seminar, Napa, USA, July 2009*, 2009.

[64] Enrique Casado, Dr Colin Goodchild, and Dr Miguel Vilaplana. Identification and Initial Characterization of Sources of Uncertainty Affecting the Performance of Future Trajectory Management Automation Systems. 2012.

[65] Gaoyang Jiang and Zhongsheng Hou. Iterative Learning Model Predictive Control Approaches for Trajectory Based Aircraft Operation with Controlled Time of Arrival. *International Journal of Control, Automation and Systems*, 18(10):2641–2649, October 2020.

[66] Joel K Klooster and David de Smedt. Controlled Time-of-Arrival Spacing Analysis. In *Proceedings of the Ninth USA/Europe Air Traffic Management Research and Development Seminar (ATM2011), Berlin, Germany*, 2011.

[67] David de Smedt, Jesper Bronsvoort, and Greg McDonald. Controlled time of arrival feasibility analysis. In *Tenth USA/Europe Air Traffic Management Research and Development Seminar (ATM2013)*, 2013.

[68] Travis L Gaydos, Worth Kirkman, Sanjiv Shresta, Eric Blair, and John Kuchenbrod. Measured variability and uncertainty in flight operations. In *2012 Integrated Communications, Navigation and Surveillance Conference*, Herndon, VA, USA, April 2012. IEEE.

[69] Travis Gaydos, Lesley A. Weitz, and Worth Kirkman. Stochastic Optimal Control for Ground-Based Metering Operations. *Journal of Air Transportation*, 24(2):29–40, April 2016.

[70] Dun Yuan Tan, Sandeep Badrinath, and Hamsa Balakrishnan. Analysis and design of Trajectory-Based Operations under wind forecast uncertainty. *CEAS Aeronautical Journal*, March 2021.

[71] Julien Scharl, Janet King, Aslaug Haraldsdottir, Rolan Shomber, and Keith Wichman. A Fast-Time Required Time of Arrival (RTA) Model for Analysis of 4D Arrival Management Concepts. In *AIAA Modeling and Simulation Technologies Conference and Exhibit*, Honolulu, Hawaii, August 2008. American Institute of Aeronautics and Astronautics.

[72] Yuyang Jia and Kaiquan Cai. The Trade-off Between Trajectory Predictability and Potential Fuel Savings for Continuous Descent Operations. In *2018 IEEE/AIAA 37th Digital Avionics Systems Conference (DASC)*, London, September 2018. IEEE.

[73] Dongdong Gui, Meilong Le, Zhouchun Huang, Junfeng Zhang, and Andrea D'Ariano. Optimal aircraft arrival scheduling model based on continuous descent operation in busy TMAs. 2021.

[74] Longbiao Ma, Yungang Tian, Yang Zhang, and Pei Chu. Trajectory Optimization of Aircraft for A Continuous Descent Continuous Procedure. In *2020 Chinese Automation Congress (CAC)*, pages 2063–2067, Shanghai, China, November 2020. IEEE.

[75] Manuel Fernando Soler Arnedo. *Commercial Aircraft Trajectory Planning based on Multiphase Mixed-Integer Optimal Control*. PhD thesis, Universidad Rey Juan Carlos, 2013.

[76] Sang Gyun Park and John-Paul Clarke. Optimal Control Based Vertical Trajectory Determination for Continuous Descent Arrival Procedures. *Journal of Aircraft*, 52(5):1469–1480, September 2015.

[77] Sang Gyun Park and John-Paul Clarke. Vertical Trajectory Optimization to Minimize Environmental Impact in the Presence of Wind. *Journal of Aircraft*, 53(3):725–737, May 2016.

[78] Laurel Stell. Prediction of top of descent location for idle-thrust descents. In *9th USA/Europe Air Traffic Management R&D Seminar, Berlin, Germany*, 2011.

[79] Ramon Dalmau Codina and Xavier Prats Menéndez. How much fuel and time can be saved in a perfect flight trajectory? continuous cruise climbs vs. conventional operations. In *Proceedings of the 6th International Congress on Research in Air Transportation (ICRAT)*, 2014.

[80] Shumpei Kamo, Judith Rosenow, Hartmut Fricke, and Manuel Soler. Robust CDO Trajectory Planning under Uncertainties in Weather Prediction. In *Proceedings of the the 13th USA/Europe Air Traffic Management Research and Development Seminar, Saclay, France*, 2019.

[81] Shumpei Kamo, Judith Rosenow, and Hartmut Fricke. CDO Sensitivity Analysis for Robust Trajectory Planning under Uncertain Weather Prediction. In *2020 AIAA/IEEE 39th Digital Avionics Systems Conference (DASC)*, San Antonio, TX, USA, October 2020. IEEE.

[82] Shumpei Kamo, Judith Rosenow, Hartmut Fricke, and Manuel Soler. Fundamental Framework to Plan 4D Robust Descent Trajectories for Uncertainties in Weather Prediction. *Aerospace*, 9(2):109, February 2022.

[83] Yoshinori Matsuno, Takeshi Tsuchiya, Jian Wei, Inseok Hwang, and Naoki Matayoshi. Stochastic optimal control for aircraft conflict resolution under wind uncertainty. *Aerospace Science and Technology*, 43:77–88, June 2015.

[84] Ramon Dalmau, Xavier Prats, and Brian Baxley. Using Broadcast Wind Observations to Update the Optimal Descent Trajectory in Real-Time. *Journal of Air Transportation*, 28(3):82–92, July 2020.

[85] Stanley Förster, Judith Rosenow, Martin Lindner, and Hartmut Fricke. A toolchain for optimizing trajectories under real weather conditions and realistic flight performance. *Greener Aviation, Brussels*, 2016.

[86] Martin Lindner, Judith Rosenow, Thomas Zeh, and Hartmut Fricke. In-Flight Aircraft Trajectory Optimization within Corridors Defined by Ensemble Weather Forecasts. *Aerospace*, 7(10):144, October 2020.

[87] Sang Gyun Park and John-Paul Clarke. Vertical Trajectory Optimization for Continuous Descent Arrival Procedure. In *AIAA Guidance, Navigation, and Control Conference*, Minneapolis, Minnesota, August 2012. American Institute of Aeronautics and Astronautics.

[88] Sang Gyun Park and J. B. Clarke. Fixed RTA fuel optimal profile descent based on analysis of trajectory performance bound. In *2012 IEEE/AIAA 31st Digital Avionics Systems Conference (DASC)*, Williamsburg, VA, October 2012. IEEE.

[89] Richard Sopjes, Paul De Jong, Clark Borst, René van Paassen, and Max Mulder. Continuous descent approaches with variable flight-path angles under time constraints. In *AIAA Guidance, Navigation, and Control Conference*, page 6219, 2011.

[90] Shih-Yih Young and Kristen Jerome. RTA-compliant optimized profile descents with 4-D FMS. In *2014 Integrated Communications, Navigation and Surveillance Conference (ICNS) Conference Proceedings*, Herndon, VA, USA, April 2014. IEEE.

[91] Shih-Yih Ryan Young, Kristen Jerome, and Rockwell Collins. Fuel-efficient optimized profile descents with time control. In *2015 Integrated Communication, Navigation and Surveillance Conference (ICNS)*, Herdon, VA, USA, April 2015. IEEE.

[92] Ramon Dalmau, Ronald Verhoeven, Nico de Gelder, and Xavier Prats. Performance comparison between TEMO and a typical FMS in presence of CTA and wind uncertainties. In *2016 IEEE/AIAA 35th Digital Avionics Systems Conference (DASC)*, Sacramento, CA, USA, September 2016. IEEE.

[93] Ramon Dalmau, Xavier Prats, Ronald Verhoeven, Frank Bussink, and Bart Heesbeen. Performance comparison of guidance strategies to accomplish RTAs during a CDO. In *2017 IEEE/AIAA 36th Digital Avionics Systems Conference (DASC)*, St. Petersburg, FL, September 2017. IEEE.

[94] Ramon Dalmau, Xavier Prats, and Brian Baxley. Fast sensitivity-based optimal trajectory updates for descent operations subject to time constraints. In *2018 IEEE/AIAA 37th Digital Avionics Systems Conference (DASC)*, pages 1–10, London, September 2018. IEEE.

[95] Raul Saez, Ramon Dalmau, and Xavier Prats. Optimal assignment of 4D close-loop instructions to enable CDOs in dense TMAs. In *2018 IEEE/AIAA 37th Digital Avionics Systems Conference (DASC)*, London, September 2018. IEEE.

[96] Raúl Sáez García and Xavier Prats Menéndez. Comparison of fuel consumption of continuous descent operations with required times of arrival. In *ICRAT 2020: papers & presentations*, 2020.

[97] P. M. A. de Jong, N. de Gelder, R. P. M. Verhoeven, F. J. L. Bussink, R. Kohrs, M. M. van Paassen, and M. Mulder. Time and Energy Management During Descent and Approach: Batch Simulation Study. *Journal of Aircraft*, 52(1):190–203, January 2015.

[98] P. M. A. de Jong, F. J. L. Bussink, R. P. M. Verhoeven, N. de Gelder, M. M. van Paassen, and M. Mulder. Time and Energy Management During Approach: A Human-in-the-Loop Study. *Journal of Aircraft*, 54(1):177–189, January 2017.

[99] Santi Vilardaga and Xavier Prats. Operating cost sensitivity to required time of arrival commands to ensure separation in optimal aircraft 4D trajectories. *Transportation Research Part C: Emerging Technologies*, 61:75–86, December 2015.

[100] Yi Cao, Sivakumar Rathinam, and Dengfeng Sun. A rescheduling method for conflict-free continuous descent approach. In *AIAA Guidance, Navigation, and Control Conference*, page 6218, 2011.

[101] Raúl Sáez García, Xavier Prats Menéndez, Tatiana Polishchuk, Valentin Polishchuk, and Christiane Schmidt. Automation for separation with cdos: dynamic aircraft arrival routes. In *Proceedings of the 13th USA/Europe Air Traffic Management Research and Development Seminar*, 2019.

[102] Heng Chen and Senay Solak. Lower Cost Arrivals for Airlines: Optimal Policies for Managing Runway Operations under Optimized Profile Descent. *Production and Operations Management*, 24(3):402–420, March 2015.

[103] Heng Chen and Senay Solak. Optimal metering policies for optimized profile descent operations at airports. In *Proc. of 6th International Conference on Research in Air Transportation, Istanbul, Turkey*, 2014.

[104] Lesley A Weitz. Derivation of a point-mass aircraft model used for fast-time simulation. Technical report, MITRE Corporation, 2015.

[105] José Pinto Peixoto and Abraham H Oort. *Physics of climate*. New York, NY (United States); American Institute of Physics, 1992.

[106] Junzi Sun, Jacco M Hoekstra, and Joost Ellerbroek. OpenAP: An open-source aircraft performance model for air transportation studies and simulations. *Aerospace*, 7(8), 2020.

[107] Devakumar Thammisetty. Development of a multi-phase optimal control software for aerospace applications (mpopt). Master's thesis, Lausanne, EPFL, 2020.

[108] Angela Nuic, Damir Poles, and Vincent Mouillet. BADA: An advanced aircraft performance model for present and future ATM systems. *International Journal of Adaptive Control and Signal Processing*, 24(10):850–866, August 2010.

[109] Worth Kirkman, Travis L. Gaydos, and Lesley A. Weitz. Optimizing Metering for Trajectory Timing Uncertainty. In *AIAA Guidance, Navigation, and Control Conference*, National Harbor, Maryland, January 2014. American Institute of Aeronautics and Astronautics.

[110] Flightaware. https://flightaware.com. Accessed: 04.25.2022.